



Quality by design (QbD) approach for developing agglomerates containing racecadotril and loperamide hydrochloride by crystallo-co-agglomeration



Kevin C. Garala ^{a,*}, Jaydeep M. Patel ^a, Anjali P. Dhingani ^a, Abhay T. Dharamsi ^b

^a Department of Pharmaceutics, Atmiya Institute of Pharmacy, Rajkot – 360005, India

^b Department of Pharmaceutics, Maliba Pharmacy College, Surat – 394 350, India

ARTICLE INFO

Article history:

Received 8 April 2013

Received in revised form 24 June 2013

Accepted 7 July 2013

Available online 20 July 2013

Keywords:

Principal component analysis

Design of experiment

Agglomerative hierarchy cluster analysis

Crystallo-co-agglomeration

ABSTRACT

This research presents the use of experimental design, optimization and multivariate techniques to investigate the root-cause of agglomerates containing two drugs [i.e. racecadotril (RCD) and loperamide hydrochloride (LPM)]. The influence of various excipients and processing conditions on formation of directly compressible agglomerates was prepared by crystallo-co-agglomeration (CCA) technique and evaluated. Design of experimental (DoE) was carried out to evaluate the interactions and effects of the design factors on critical quality attributes (CQAs) of agglomerates. The design space was studied by DoE and multivariate analysis to ensure desired physico-chemical properties of agglomerates. The overall higher yield of the process with sufficient size of agglomerates was prepared by CCA. The optimized agglomerates exhibited excellent flowability and crushing strength along with good compressibility and compactibility. The optimized batch of agglomerates was characterized by Fourier transform infrared spectroscopy, differential scanning calorimetry, powder X-ray diffractometry and gas chromatography which illustrated the absence of drug–excipient interaction with minimal entrapment of solvent. It was demonstrated that QbD principles and tools provide an effective means to achieve a greater understanding of agglomerates prepared by CCA which adopted as an excellent alternative to wet granulation.

© 2013 Elsevier B.V. All rights reserved.

1. Introduction

The United States (US) Food and Drug Administration (FDA) published a concept paper on current good manufacturing practices (cGMP) for the 21st century [1]. This article expressed a desire that companies build quality, safety and efficacy into their new products as early as possible. This concept became well recognized as Quality by Design (QbD). Key to successfully executing QbD approach is distinguishing those characteristics of products that are critical to its safety, efficacy and quality, i.e. critical quality attributes (CQAs), plus those aspects of processes that impact those product characteristics, i.e. critical process parameters (CPPs) [2]. Often design of experiment (DoE) exercised in the context of QbD, which requires a multivariate approach for understanding the multifactorial relationships among formulation parameters. To improve process knowledge, statistical DoE is a valuable tool to establish in mathematical form the relationships between CPPs and CQAs [3–5].

A range for each process parameter and their combinations can be defined, in which the desired CQAs are achieved. All likely combinations of raw material attributes and process parameters that need to be realized by the process, to ensure that the CQAs stay within the required ranges (control space), can be called the “design space” of the process. The “design space” can be then defined, allowing an in-depth understanding of the problem and, sequentially, the maintaining of the product final quality [6].

Multivariate tools, such as principal component analysis (PCA), offer opportunities to more effectively and efficiently describe CQAs. By using a statistical multivariate data analysis, e.g. PCA, on a set of experimental data, it is possible to reveal intrinsic structures and to group observations in the data, which might be difficult to do by traditional univariate data analysis [7]. PCA is a method of data reduction and classification that transforms highly correlated, multidimensional data into a new system of variables called principal components. These new variables, which are linear combinations of the original variables, are selected so that they explain as much of the original data's variability as possible. Each principal component (PC) is uncorrelated and orthogonal to all other PCs. The first principal component (PC1) is oriented in the direction of maximum variability. Principal component 2 (PC2) is orthogonal to PC1 and captures the second largest variation in the data set. Therefore, each PC represents a source of variability that is

* Corresponding author at: Atmiya Institute of Pharmacy, Yogidham Gurukul, Kalawad Road, Rajkot – 360005, India. Tel.: +91 9974664666; fax: +91 281 2563766.

E-mail addresses: kevincgarala@gmail.com (K.C. Garala), jmpatel7@gmail.com (J.M. Patel), anjali.patel27@gmail.com (A.P. Dhingani), aadharamsi@gmail.com (A.T. Dharamsi).

independent of the other sources. In the case of compaction data, one can imagine that a property, such as plasticity, is associated with some fraction of the variability observed in solid fraction and mechanical energy consumption between materials. Therefore, the principal components are expected to reflect distinct mechanical and physical behaviors, which were convoluted together in the original multivariate data [8]. Furthermore, PCA combined with an agglomerative hierarchical cluster analysis (AHCA) based on the similarity or dissimilarity of whole cases to describe a set of multivariate methods and techniques that seek to classify data, often into profiles, groups, types, and so on [9].

Drugs with poor compressibility and flowability are unsuitable for the direct compression. Particle size enlargement techniques employed in the field of pharmacy in order to improve flowability of compression blend include melt granulation [10], extrusion-spheronization [11], melt solidification [12], melt extrusion [13], and spherical crystallization [14]. Among all, spherical crystallization technique is supposed to modify crystal nature and produces directly compressible agglomerates. Moreover, apart from modifications in the primary and secondary properties of the particles, this technique also offers advantages in terms of reduction in the number of unit operations and in turn, processing cost. The suitability of this technique relies on the desired properties of the enlarged particle and the physico-chemical properties of the drug and excipients utilized. The unsuitability of SC for low-dose and combination of drugs, Kadam et al. [15] has been successfully overcome by crystallo-co-agglomeration (CCA) technique. CCA, a novel particle engineering technique, is a modification of a SC in which a drug is crystallized and agglomerated with an excipient(s) or with another drug, which may or may not be crystallized in the system.

The present research work was aimed to develop agglomerates containing racecadotril (RCD) and loperamide hydrochloride (LPM) by CCA technique. The long needle like crystalline properties of RCD produces poor flowability and compressibility which ultimately cause difficulty in direct compression [16]. Agglomerates containing 100 mg RCD and 4 mg LPH were developed since the combination seems as effective as high-dose of individual drug [17]. Furthermore, RCD is insoluble in water and this makes a rapid release of molecule by disintegration of the tablet more difficult [16]. Hence, the current research work was mainly focused on the influence of processing condition and various excipients on the formation of agglomerates of combined drugs (RCD and LPM) and its mechanical properties in order to obtain excellent flowability and compressibility for direct compression. In order to optimize agglomerates, principal component analysis (PCA), agglomerative hierarchy cluster analysis (AHCA), and 3^2 full factorial experimental design were implemented.

2. Materials

RCD was procured from Ogene Systems (I) Pvt. Ltd., Hyderabad, India. LPM was obtained from Torrent Research Center, Gandhinagar, India. Talc, PEG 6000 and PVA were purchased from HiMedia Labs, Mumbai, India. HPMC was gifted by Colorcon Asia Pvt. Ltd., Goa, India. High performance liquid chromatography (HPLC) grade acetonitrile and water were purchased from Merck Pvt. Ltd., Mumbai, India. All other chemicals used were of analytical grade (Merck Pvt. Ltd., Mumbai, India) and double distilled water was utilized throughout the study.

3. Methods

3.1. Preparation of agglomerates

3.1.1. Selection of solvent systems

A wide range of solvents were screened with different polarity for selection of good solvent and poor solvent. An excess amount of RCD and LPM was added to each of selected 5 mL solvent. All these saturated solutions were kept for 24 h in a cryostatic constant temperature reciprocating shaker bath (Tempo Instruments and Equipments Pvt.

Ltd., Mumbai, India) at a temperature of 25 ± 1 °C with constant shaking at 120 rpm [18,19]. The concentration of drugs in each sample was determined by HPLC method (Shimadzu, Japan). The study was repeated in triplicates in order to estimate reproducibility of results.

3.1.2. Crystallization procedure

On the basis of solubility study, good solvent and poor solvent was identified for the preparation of agglomerates by CCA technique. In crystallization vessel, as described by Morishima et al. [20], RCD and LPM were dissolved in good solvent followed by talc (1%w/w) and PVA (2%w/w). 100 mL of poor solvent with 1%w/w HPMC E50 LV and PEG 6000 (Table 1) was added to crystallization vessel and these contents were stirred at specific speed by using four blade mechanical stirrer. On the basis of solubility data of LPM the external phase was saturated with drug prior to formulation in order to avoid any drug loss. The stirring was continued until the mixture appeared clear at top along with settling of agglomerates. The agglomerates generated were filtered and dried overnight at room temperature. The dried agglomerates were stored in screw-capped jars at room temperature before to be evaluated. The effect of different concentrations of excipients was investigated and optimized [19].

3.2. Experimental design

Three level, two factor full factorial design was implemented to evaluate main effects and interaction effects of the formulation ingredients on the various properties of agglomerates containing RCD and LPM in order to optimize the formulation. The non-linear quadratic model generated by the design is as follows:

$$Y_i = b_0 + b_1X_1 + b_2X_2 + b_{12}X_1X_2 + b_{11}X_1^2 + b_{22}X_2^2 \quad (1)$$

where, Y_i was the dependent variable, b_0 was the arithmetic mean of nine runs and b_i was the estimated coefficient for factor X_i . The main effects (X_1 and X_2) represent average result of changing one factor at a time from its low to high value whereas the interaction term (X_1X_2) prompt change in responses when two factors were simultaneously altered. The polynomial terms (X_1^2 and X_2^2) were included to investigate the nonlinearity of the model developed [21]. A three-level two-factor, full factorial design was generated by an experimental design software SYSTAT version 12.02.00 (SYSTAT Software Inc., Chicago, USA). Based on preliminary trials, independent variables (factors) were determined as; amount of good solvent (X_1) and concentration of polymer (X_2). The formulation composition of agglomerates is summarized in Table 1.

Table 1
 3^2 full factorial design batches.

Batch code	Independent variables		
	X_1^a	X_2^b	
RL1	−1	−1	
RL2	0	−1	
RL3	1	−1	
RL4	−1	0	
RL5	0	0	
RL6	1	0	
RL7	−1	1	
RL8	0	1	
RL9	1	1	
Factor	Level		
	−1	0	1
X_1 (Amount of DCM, mL)	4	7	10
X_2 (Concentration of PEG, %w/w)	2	3.5	5

^a X_1 : Amount of DCM, mL.

^b X_2 : Concentration of PEG, %w/w.

Table 2
Results of evaluation parameters of pure drugs and agglomerates.

Batch ^a	dg ^b	SF ^c	CI ^d	CS ^e	%Y ^f	AoR ^g	HR ^h	CF ⁱ	IF ^j	Φ ^k	MC ^l	K ^m	a ⁿ	1/b ⁿ	A ^o	k ^o	Py ^o	σ ₀ ^o	ER ^p	TS ^q	DCR ^r	DCL ^s
RL	0.226 ± 0.182	0.374 ± 0.049	38.73 ± 2.85	–	–	45.07 ± 3.11	1.599 ± 0.153	0.338 ± 0.094	1.982 ± 0.097	0.072 ± 0.033	0.319 ± 0.124	0.078 ± 0.025	0.416 ± 0.067	16.845 ± 1.29	1.128 ± 0.084	0.035 ± 0.016	28.43 ± 1.71	9.458 ± 1.08	4.429 ± 0.507	1.645 ± 0.197	–	–
RL1	0.497 ± 0.153	0.788 ± 0.071	19.24 ± 1.27	38.75 ± 2.15	92.24 ± 2.24	24.23 ± 1.47	1.185 ± 0.019	1.159 ± 0.127	2.385 ± 0.058	0.855 ± 0.082	0.933 ± 0.173	0.945 ± 0.097	0.108 ± 0.017	8.854 ± 0.437	0.722 ± 0.061	0.815 ± 0.112	1.271 ± 0.12	0.408 ± 0.14	0.819 ± 0.128	4.948 ± 0.471	98.76 ± 1.52	99.37 ± 2.05
RL2	0.748 ± 0.086	0.821 ± 0.057	16.81 ± 1.89	57.13 ± 2.94	94.36 ± 2.41	18.59 ± 1.45	1.235 ± 0.022	0.976 ± 0.162	2.831 ± 0.072	0.956 ± 0.091	0.914 ± 0.186	0.971 ± 0.109	0.157 ± 0.016	5.385 ± 0.529	0.838 ± 0.042	0.586 ± 0.076	1.706 ± 0.08	0.568 ± 0.19	0.702 ± 0.115	4.796 ± 0.529	97.07 ± 1.48	97.75 ± 1.33
RL3	0.923 ± 0.129	0.811 ± 0.074	17.59 ± 2.05	45.36 ± 2.57	90.28 ± 2.52	20.95 ± 1.04	1.166 ± 0.017	0.972 ± 0.173	2.597 ± 0.061	0.865 ± 0.097	0.8468 ± 0.163	0.982 ± 0.084	0.142 ± 0.018	4.383 ± 0.511	0.605 ± 0.039	0.427 ± 0.083	2.341 ± 0.15	0.786 ± 0.21	0.753 ± 0.134	5.142 ± 0.582	99.75 ± 1.72	97.34 ± 1.72
RL4	0.672 ± 0.137	0.884 ± 0.062	18.75 ± 2.11	50.92 ± 3.17	89.35 ± 3.74	21.87 ± 1.52	1.209 ± 0.018	0.985 ± 0.138	2.483 ± 0.091	0.923 ± 0.101	0.925 ± 0.148	1.054 ± 0.117	0.155 ± 0.015	5.856 ± 0.573	0.916 ± 0.077	0.633 ± 0.091	2.577 ± 0.16	1.024 ± 0.15	0.601 ± 0.129	5.972 ± 0.621	96.61 ± 1.84	98.65 ± 1.43
RL5	0.821 ± 0.162	0.915 ± 0.078	15.93 ± 1.43	53.34 ± 2.41	96.38 ± 2.17	19.31 ± 1.54	1.119 ± 0.015	0.972 ± 0.151	2.783 ± 0.059	0.959 ± 0.112	0.912 ± 0.141	0.972 ± 0.098	0.148 ± 0.013	3.058 ± 0.371	0.728 ± 0.045	0.731 ± 0.089	2.369 ± 0.19	0.856 ± 0.19	0.791 ± 0.153	6.261 ± 0.497	97.52 ± 1.91	99.52 ± 1.97
RL6	0.962 ± 0.175	0.917 ± 0.069	16.72 ± 1.18	56.53 ± 3.28	92.95 ± 2.49	20.09 ± 1.95	1.152 ± 0.018	0.988 ± 0.126	3.014 ± 0.121	0.972 ± 0.083	0.907 ± 0.118	0.942 ± 0.115	0.128 ± 0.014	5.193 ± 0.543	0.749 ± 0.033	0.671 ± 0.107	2.491 ± 0.12	0.926 ± 0.22	0.725 ± 0.173	4.925 ± 0.574	98.14 ± 1.78	97.81 ± 1.95
RL7	0.907 ± 0.094	0.946 ± 0.073	17.63 ± 2.14	45.26 ± 2.41	97.32 ± 3.05	21.61 ± 2.19	1.183 ± 0.014	0.998 ± 0.172	2.637 ± 0.083	0.969 ± 0.125	1.292 ± 0.225	0.963 ± 0.079	0.142 ± 0.018	4.298 ± 0.509	0.823 ± 0.053	0.669 ± 0.072	2.492 ± 0.16	0.847 ± 0.23	0.522 ± 0.132	5.986 ± 0.541	97.09 ± 2.11	99.47 ± 1.64
RL8	1.075 ± 0.105	0.978 ± 0.043	14.27 ± 1.02	60.25 ± 3.06	91.74 ± 2.59	19.52 ± 1.56	1.112 ± 0.016	1.069 ± 0.135	3.045 ± 0.084	0.993 ± 0.072	0.992 ± 0.207	0.957 ± 0.083	0.151 ± 0.016	2.806 ± 0.385	0.721 ± 0.043	0.535 ± 0.093	1.869 ± 0.11	0.622 ± 0.11	0.593 ± 0.141	6.137 ± 0.672	100.04 ± 1.52	96.83 ± 1.17
RL9	0.944 ± 0.148	0.963 ± 0.061	16.29 ± 1.91	41.29 ± 2.19	93.37 ± 2.84	19.74 ± 1.38	1.169 ± 0.017	1.124 ± 0.152	2.912 ± 0.076	0.975 ± 0.064	1.154 ± 0.156	0.977 ± 0.094	0.145 ± 0.014	4.945 ± 0.612	0.769 ± 0.057	0.764 ± 0.087	2.308 ± 0.12	0.834 ± 0.17	0.638 ± 0.139	6.058 ± 0.523	99.82 ± 1.28	98.64 ± 1.55

^a Results are mean of three determinations ±

SD.

^b Mean geometric diameter.

^c Shape factor.

^d Carr's index.

^e Crushing strength.

^f Percent yield.

^g Angle of repose.

^h Hausner ratio.

ⁱ Circularity factor.

^j Irregularity factor.

^k Aspect ratio.

^l Moisture content.

^m Kuno's constant.

ⁿ Kawakita parameters.

^o Heckel parameters.

^p Elastic recovery.

^q Tensile strength.

^r RCD content.

^s LPM content.

Additionally the composition of optimized (check point) batch was derived by constructing overlay plot. The percentage relative error of each response was calculated using the following equation in order to judge the validity of the model [22–24].

$$\% \text{ Relative Error} = \frac{|\text{Predicted value} - \text{Experimental value}|}{\text{Predicted value}} \times 100 \quad (2)$$

3.3. Characterization of agglomerates

3.3.1. Drug content and percent yield

Drug content is the ratio of experimentally measured drug content to the theoretical value, expressed as percentage (%). Accurately weighed quantity of prepared agglomerates was dissolved in a sufficient quantity of a suitable solvent in which they were easily soluble. These solutions were appropriately diluted and drug content was determined by previously validated HPLC method. The percent (%) yield of samples was calculated using following Eq. (3). The average of three determinations was considered as mean value for both parameters [25].

$$\% \text{ Yield} = \frac{\text{Total weight of agglomerates}}{\text{Total weight of drug and excipients}} \times 100 \quad (3)$$

3.3.2. Size analysis

The size of pure drug particles and prepared agglomerates was measured by optical microscope (MLX-DX, Olympus (I) Pvt. Ltd., New Delhi, India). The size of randomly selected particles or agglomerates was measured and their mean geometric diameter (dg) was calculated [26].

3.3.3. Shape analysis

Shape parameters of pristine RCD and LPM as well as prepared agglomerates were evaluated based on the projected images of randomly positioned particles. The photomicrographs of the randomly selected agglomerates were taken using CCD camera (MIPS-USB, Olympus (I) Pvt. Ltd., New Delhi, India) and tracings of the enlarged photomicrographs were used for the measurement of length, width, area and perimeter. Numerous shape descriptors like; aspect ratio (AR), shape factor (SF), circularity factor (CF) and irregularity factor (IF) were evaluated as per Eqs. (4), (5), (6) and (7), respectively. Results of each parameters were the average of three determinations.

$$\text{AR} = b/l \quad (4)$$

where, b and l are the minor and major axes of traced photograph respectively.

$$\text{SF} = P'/P \quad (5)$$

where, $P' = 2\pi(A/\pi)^{1/2}$, A and P are the area and perimeter of the projected photograph respectively.

$$\text{CF} = (P')^2/4\pi A \quad (6)$$

$$\text{IF} = P/l \quad (7)$$

3.3.4. Flow parameters

Angle of repose (AoR) was determined using fixed funnel method [27]. Percentage compressibility (Carr's Index, CI) [28] and Hausner's ratio (HR) [29] were calculated after tapping fixed amount of agglomerates using tap density apparatus (ETD 1020, Electrolab,

Mumbai, India). The average of three determinations was considered as final results.

3.3.5. Measurement of packability

3.3.5.1. *Kawakita analysis.* The packing ability of the samples was investigated by tapping them into a measuring cylinder using a tap density apparatus (ETD 1020, Electrolab, Mumbai, India). The packability was calculated by the following equation [30].

$$\frac{n}{C} = \frac{1}{ab} + \frac{n}{a} \quad (8)$$

where, a and b are the constants, n is the tap number, and C denotes the volume reduction which again calculated according to the following equation

$$C = \frac{V_0 - V_n}{V_0} \quad (9)$$

where, V_0 and V_n are the powder or agglomerate bed volumes at initial and n th tapped state, respectively. The average of three determinations was considered as the mean of individual Kawakita parameters.

3.3.5.2. *Kuno analysis.* The relationship between the change in apparent density and the number of tappings was described by Kuno as per following equation [31].

$$\ln(\rho_t - \rho_n) = -Kn + \ln(\rho_t - \rho_0) \quad (10)$$

where, ρ_t is the apparent density at infinite taps, ρ_n is the apparent density at n th tapped state, ρ_0 is the apparent density at initial cascade state and the constant K represents the rate of packing process under tapping [32].

3.3.5.3. *Heckel analysis.* Accurately weighed quantity of samples of pure drugs as well as agglomerates was compressed by hydraulic press (TechnoSearch Instrument, Mumbai, India) at the constant compression with different pressures and a dwell time of 1 min [33]. Before compression, lubrication of die and punches was carried out by 1% w/v dispersion of magnesium stearate in acetone. Compacts were allowed to relax for 24 h at ambient temperature and the data obtained was subject to Heckel plot using the following equation [34,35].

$$\ln \frac{1}{1-D} = kPy + A \quad (11)$$

where, D is relative density of compacts i.e. ratio of compact density to true density of powder, P is the applied compression pressure, and k and A are constants. The reported mean yield pressures, P_y , are the reciprocal of the slope k , which was calculated using linear regression in a pressure range determined separately for each material. k is equal to $1/3\sigma_0$, where, σ_0 is the yield strength and $3\sigma_0$ is the mean yield pressure (P_y). Here, the density of prepared compacts for Heckel parameter was calculated from the volume of compacts and mass of compacts. The average of three determinations was considered as the mean of respective Heckel parameters.

3.3.6. Tensile strength

The radial tensile strength (σ_r) of compacts prepared from powders or agglomerates is considered as force per unit area of broken face required to split a prepared compact. The data used for compressional studies of prepared agglomerates were used to study the pressure tensile strength relationship. The hardness value of compacts was

determined by a Monsanto type hardness tester and used for σ_t determination using the following equation [36]. The average of three determinations was considered as σ_t .

$$\sigma_t = \frac{2F}{\pi Dt} \quad (12)$$

where, F is the crushing force (N), D is the tablet diameter, and t is the compact thickness.

3.3.7. Elastic recovery

The compacts prepared, from pure drugs and agglomerates, for the Heckel plot study and tensile strength determination were used for the elastic recovery test. The thickness of the compacts was measured immediately after ejection (H_c) and after 24 h relaxation period (H_e). The elastic recovery was calculated by following equation [37]. The average of three determinations was considered as % ER.

$$\% ER = [(H_e - H_c)/H_c] \times 100 \quad (13)$$

3.3.8. Crushing strength

Crushing strength (CS) of prepared agglomerates was determined by mercury load cell method [38]. The agglomerate was placed inside the syringe and mercury was added through hollow syringe tube. The total weight of tube with mercury, at the stage where co-agglomerate broke, gave the measure of CS of that particular agglomerate. The average of three determinations was considered as CS.

3.3.9. Percent moisture content

Moisture content (MC) of prepared agglomerates was determined by IR moisture balance (Rajdhani, Mumbai, India). The agglomerates (5 g) were separately placed in heating pan and heated at a temperature 105 °C for 4 h. The percent reduction in the weight of agglomerates due to moisture loss was directly displayed on the scale. The average of three determinations was considered as % MC.

3.3.10. Scanning electron microscopy

The shape and surface morphology of pure drugs and prepared agglomerates were observed using scanning electron microscope (SEM) (JEOL, JSM 5610 LV, Japan). The agglomerates were observed at various magnifications in order to analyze the effect of additives on surface morphology and agglomeration efficiency.

3.3.11. Fourier transform-infrared (FT-IR) spectroscopy

Infrared spectra of pure drugs and optimized agglomerates were recorded using infrared spectrophotometer (Nicolet iS10, Thermo Fisher Scientific Inc., USA). The samples were dispersed in KBr and compressed into disk by the application of pressure using hydraulic press. The pellets were placed in the sample holder and FT-IR spectra were recorded over the range of 400–4000 cm^{-1} .

3.3.12. Differential scanning calorimeter (DSC) analysis

DSC spectra of pure drugs, polymers and optimized agglomerates were recorded using differential scanning calorimeter (DSC-60, Shimadzu, Tokyo, Japan) which was previously calibrated with indium standard. Sample (~5–10 mg) was hermetically sealed in an aluminum crucible and subjected to a purging of nitrogen gas at a flow rate of 50 mL/min. The heating was done at a rate of 10 °C/min. Empty sealed aluminum pan was used as reference [39,40]. The spectra obtained were analyzed for endothermic and exothermic transitions in drug agglomerates [41]. The crystallinity (X_{cr}) was calculated as;

$$X_{cr} = \frac{\Delta H}{\Delta H_0} \quad (14)$$

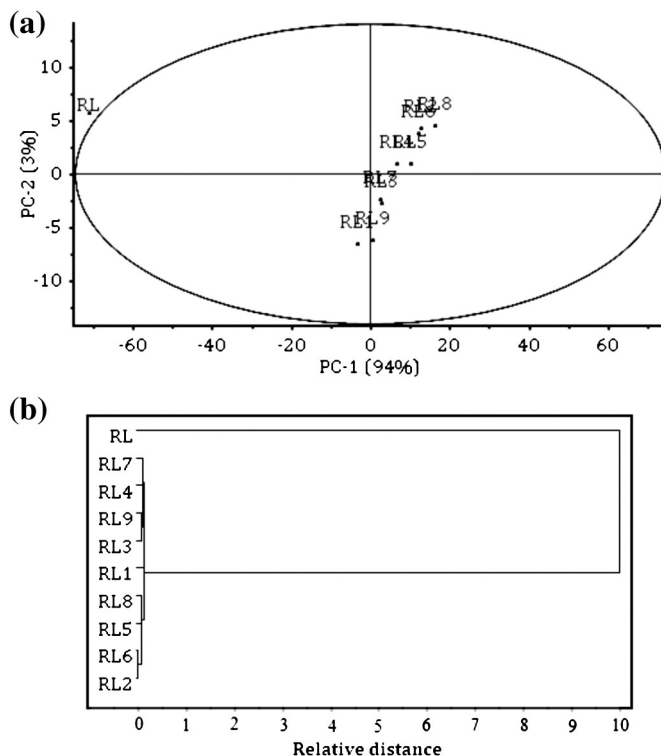


Fig. 1. (a) Score plot from PCA and (b) dendrogram from AHCA of coarse and agglomerated RL.

where, ΔH_0 and ΔH are the heat of fusion of the unprocessed and the treated crystals, respectively [42].

3.3.13. Powder X-ray diffractometry (PXRD)

The X-ray powder diffraction patterns of pure drugs and optimized agglomerates were recorded using diffractometer system (X'Pert MPD, Philips, Netherlands) with a copper target and scintillation counter detector (voltage 40 kV; current 30 mA; and scanning speed 0.05°/s). The sample holder was non-rotating and the temperature of acquisition was at room temperature. The diffraction pattern was analyzed for the 2 θ range from 10° to 90° [43].

3.3.14. Gas chromatography

Accurately weighed optimized agglomerates were suspended in methanol and shaken in orbital shaking incubator (Remi Laboratory Instruments, Mumbai, India) for 24 h at 100 rpm. Subsequently, the dispersion was filtered and filtrate was analyzed using gas chromatography (head space) GC-HS (Turbo matrix 40, Perkin Elmer, USA) with column Rtx-5MS (thickness: 0.25 μm , diameter: 0.25 μm and length: 60 m) and Helium as carrier gas. The reference solution (1000 ppm) and sample solution were injected alternately to GC-HS and the area of peak obtained was used to calculate the solvent concentrate in agglomerates.

3.3.15. In vitro dissolution study

In vitro dissolution study for pure drugs and prepared agglomerates was performed using USP type II apparatus (TDT 06P, Electrolab, India) to evaluate an influence of various excipients on drug release from agglomerates. 900 mL of acetate buffer pH 4.5 with 0.75% SLS was used as a dissolution medium which was maintained at 37 ± 0.5 °C and stirred at 100 rpm. Aliquots of 5 mL were withdrawn at predetermined time intervals and replaced with the same amount of fresh dissolution medium. After suitable dilution the samples were analyzed by HPLC method and cumulative percentage drug release (CPR) was calculated.

3.4. Principal component analysis

Principal component analysis (PCA) was implemented to reveal latent structures in the data set and to identify the grouping of the materials using The Unscrambler® 10.2 software (CAMO AS, Norway). The data matrix included the previously described set of materials (objects, $n = 9$), each characterized by various parameters (variables, $p = 21$). PCA modeling was done using systematic cross-validation; data were centered and scaled using a common normalization method ($1/SDev$) [44]. A systematic approach was applied; first, including pure RCD and agglomerates into the model, followed by identification of extremes or potential outliers. Extreme samples were then left out in order to analyze the remaining materials in further detail.

4. Results and discussions

4.1. Principal component analysis

For all experimental design batches of agglomerates, responses like percent yield (%Y), mean geometric diameter (dg), angle of repose (AoR), Carr's index (CI), Hausner ratio (HR), drug content (DC), aspect ratio (φ), irregularity factor (IF), crushing strength (CS), shape factor (SF), circularity factor (CF), Kawakita parameters (a and 1/b), Kuno's constant (K), Heckel plot parameters (A, k, Py and σ_0), elastic recovery (ER), tensile strength (TS) and moisture content (MC) were evaluated and documented in Table 2. PCA was performed on these data set using software package The Unscrambler® 10.2 for all experimental design batches in order to scrutinize critical responses. The multivariate approach by using PCA is dating back to the beginning of the 20th century [45] and most common latent variable projection method [46]. PCA is a mathematical algorithm that reduces the dimensionality of the data while retaining most of the variation in the data set [47]. It allows the results to be simplified into latent variables (principal components) that explain the main variance in the data [48]. PCA is

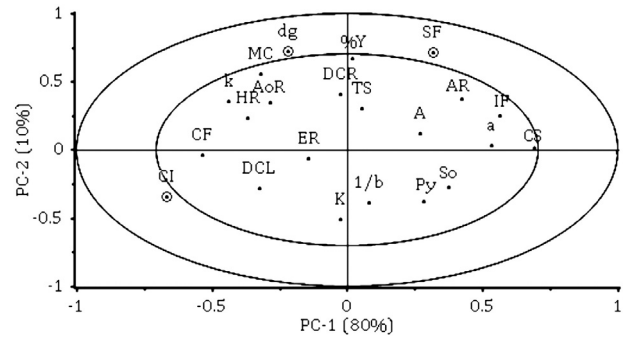


Fig. 3. Correlation loading plot obtained by PCA of RL agglomerates.

used for getting overview of data tables (their structure, similarities or dissimilarities, trends, deviating observations).

Initially, PCA was performed to examine the relationship of all properties obtained from the series of experimental design and untreated crystals of RCD and LPM (RL). Further, identification of objects for the different developmental stages was carried out by examining the scores and the loadings. The loadings are the contributions from the variables to the principal components and the scores are the contributions from the samples. The larger the loading, the more important the agglomerates for a particular PC are; and the larger the score, the more important the sample is [49].

As depicted in Fig. 1a, the first principal component (PC1) was responsible for 94% of the total variance in the data set and the second (PC2) was responsible for a further 3%; thus, the cumulative contribution was 97%. Based on the PCA score plot in Fig. 1a, RL crystals were categorized as extreme objects. The RL was separated from the agglomerates of all batches as clearly observed outside of ellipse, which was further proved by agglomerative hierarchy cluster analysis (AHCA). AHCA refers to a set of analytic procedures that reduce complex multivariate data into smaller subsets or groups [50]. Compared with other data reduction methods, AHCA yields groupings that are based on the similarity or dissimilarity of whole cases [51]. AHCA represents an important analytic tool for the health sciences and may be used to devise patient or consumer profiles, or in the development of classification systems or taxonomies. The data obtained were also classified by AHCA using the Euclidean distance (nearest neighbor method) [52]. Euclidean distances, which can reveal the relationship of two samples, are calculated by Eq. (15).

$$EUCLID = \sqrt{\sum_{i=1}^n (x_i - y_i)^2} \tag{15}$$

EUCLID is the Euclidean distances of two samples; n is the number of variables, x_i is the value of variable i of one sample, and y_i is the value of variable i of another sample. Then cluster analysis diagram (dendrogram) can be obtained by Euclidean distances [53].

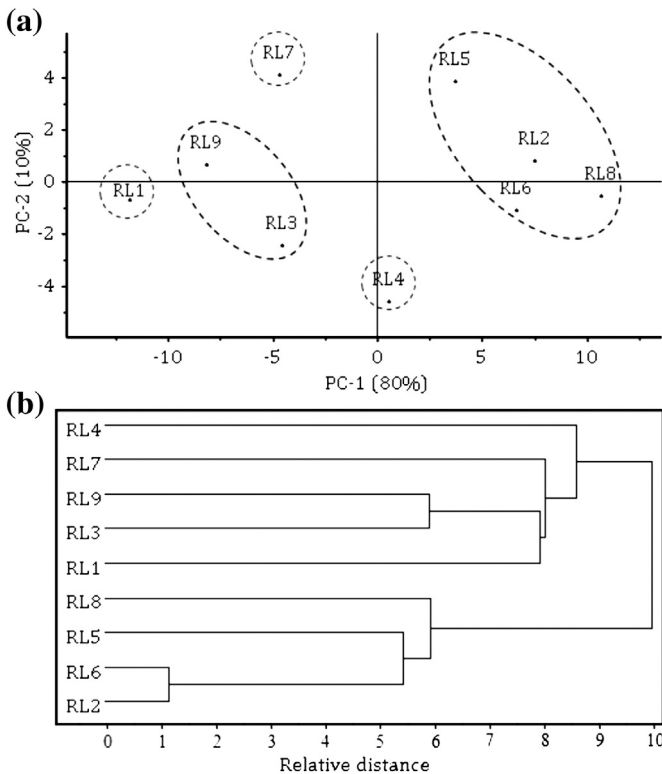


Fig. 2. (a) Score plot from PCA and (b) dendrogram from AHCA of agglomerated RL.

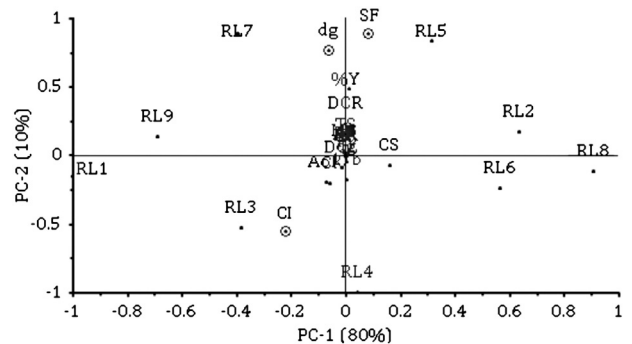


Fig. 4. Bi-plot obtained by PCA of RL agglomerates.

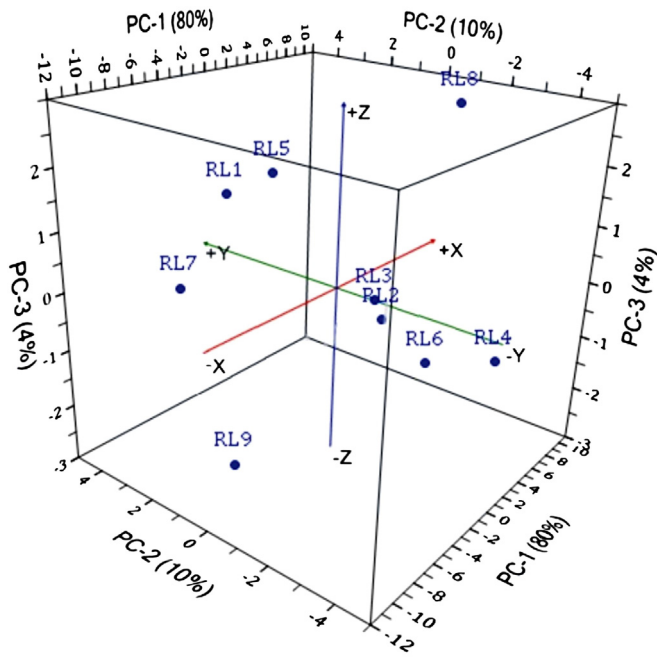


Fig. 5. PCA 3D score plot for the PC1, PC2 and PC3.

Furthermore, resulting PC scores were analyzed by a clustering approach. This approach is often considered an optimal way to perform classifications. With hierarchical average linkage, which is an agglomerative method, each samples (as represented by its component scores) initially started out as an individual cluster. Similar agglomerates were then merged, where cluster similarity was determined by the mean distance between all objects in the clusters (weighted by the number of members), until all samples were united into one cluster [54]. The AHCA results may be examined in the form of a dendrogram (a tree of clusters) and subjectively determine how many clusters appear to exist with their similarities [9].

The dendrogram, a graphical display of the result of AHCA is shown in Fig. 1b. Two major clusters found representing coarse RL and agglomerated RL batches separately with higher relative distance. It revealed that various properties of coarse RL were significantly distinctive from agglomerated RL which proved the results of PCA score plot (Fig. 1a). Therefore, RL was eliminated from the data set and a new PCA model was built without RL, as a means to better illustrate the distribution of the remaining agglomerated RL.

The PCA score plot of the all variables of all batches of full factorial design is given in Fig. 2a. The agglomerates spread out relatively homogeneously into four quartiles of the score plot and the PC1 was responsible largest variation, i.e. 80%, of the total variance in the data set, while the PC2 was responsible for a further 10%; thus, the

cumulative contribution was 90%. Further, all batches of experimental design were defined in different group by AHCA. It was used for the evaluation of the similarity and dissimilarity of all batches. As seen from Fig. 2b, all the formulations were clustered into five groups; group I (RL2, RL5, RL6 and RL8), group II (RL3 and RL9), group III (RL1), group IV (RL4) and group V (RL7). All the five groups were relatively distant and substantially different from one another.

Correlation loading plot of the first two principal components is shown in Fig. 3. In general, it is considered that variables near each other are positively correlated, while those on opposite sides of the origin are negatively correlated in loading plots. All defined properties of agglomerates were classified into the following four groups based on the origin; top, bottom, right and left. With regard to the variables dg and CS were plotted on the opposite side of the origin whereas CI was plotted in the similar side to dg on PC1. Further, SF was found to be negatively correlated with dg and CI was positively correlated with dg. This result implied that if the dg of agglomerates was increased, the SF would decrease. In addition to this, the CI and AoR were negatively correlated with SF on PC1. This finding suggested that as sphericity of agglomerated crystals increased and resulted into an improvement in flowability as the values of flow parameters (AoR and CI) decreased. Again this result correlated with the previous investigation [55]. Furthermore, other variables plotted on loading plot at low values near to origin and hence, they were not further considered for discussion. Finally, this PCA result was also considered to be reasonable and the cumulative contribution ratio of PC1 and PC2 was 90%. Correlation loading plot also decided the most important variables which are illustrated in Fig. 3. The results depicted that there were three most important variables (dg, SF and CI) marked by a circle as they were enclosed between two ellipses.

Fig. 4 shows a PCA bi-plot containing both scores and loading vectors of agglomerates. In the PCA bi-plot, CI of batches RL1, RL3, RL7 and RL9 were plotted on the same side of PC1, which depicted that they were positively correlated and hence, CI of these batches was high. Similarly, dg and SF of batches RL2, RL5, RL7 and RL9 were plotted on the same side of PC2. In Fig. 5, the third principal component (PC3), explaining an additional 4% of the variation in the data, is displayed in 3D score plot against PC1 and PC2. Due to the very low explained variation of PC3, it was not important in the development of agglomerates and hence, not further discussed. The reduced PCA model was explained with a total of 94% of the variation on the data set over three principal components (PC1: 80%; PC2: 10%; PC3: 4%).

Plotting the eigenvalues against the corresponding PC produces a scree plot that illustrated the rate of change in the magnitude of the eigenvalues for the PC. The Cattell [56] scree test and the Kaiser [57] criterion are the most frequently used procedures. They are both based on the inspection of the correlation matrix eigenvalues. Cattell's recommendation was to retain only those components above the point of inflection on a plot of eigenvalues ordered by diminishing

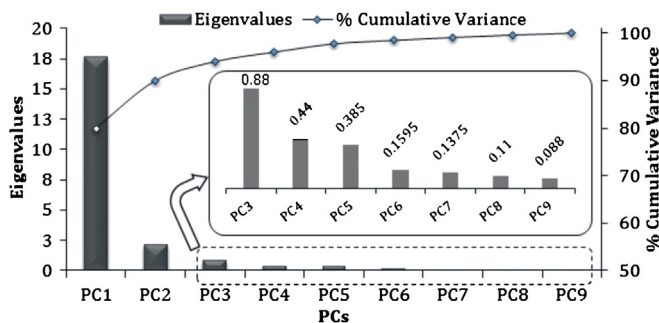


Fig. 6. Scree plot of all components with cumulative variance.

Table 3
Regression analysis of full factorial design batches of agglomerates.

Coefficients	dg (Y ₁)		SF (Y ₂)		CI (Y ₃)	
	FM ^a	RM ^b	FM	RM	FM	RM
b ₀	0.8608	0.8387	0.9188	0.9188	15.78	15.67
b ₁	0.1255	0.1255	0.0116	0.0116	-0.836	-0.836
b ₂	0.1263	0.1263	0.0778	0.0778	-0.910	-0.910
b ₁₁ ^c	-0.0638	-	-0.0191	-0.0191	2.030	2.03
b ₂₂ ^{c,e}	0.0306	-	-0.0210	-0.0210	-0.161	-
b ₁₂ ^{d,e}	-0.0972	-0.0972	-0.0020	-	0.077	-

^a FM, Full model.

^b RM, Reduced model.

^c Nonsignificant (P > 0.05) coefficients for Y₁.

^d Nonsignificant (P > 0.05) coefficients for Y₂.

^e Nonsignificant (P > 0.05) coefficients for Y₃.

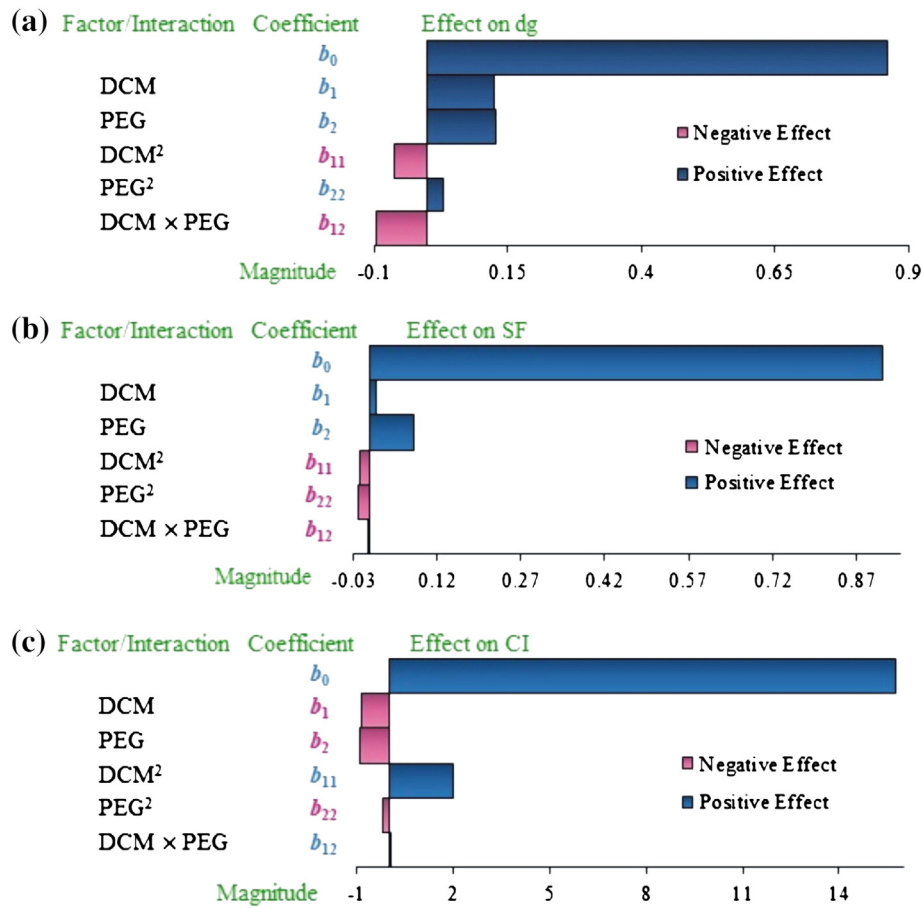


Fig. 7. Graphical representation of the magnitudes of the main effects and interactions of the factors on (a) dg; (b) SF and (c) CI of RL agglomerates.

size. Kaiser [57] recommended that only eigenvalues at least equal to one are retained as one is the average size of the eigenvalues. Eigenvalues of all PCs were calculated using XLSTAT® software version

Table 4
Calculation for testing the model in portions for agglomerates.

Model	df ^c	SS ^d	MS ^e	R ²
<i>Mean geometric diameter (Y₁)</i>				
Regression				
FM ^a	5	0.23812	0.04762	0.9641
RM ^b	3	0.22809	0.07603	0.9234
Residual				F _{cal} = 1.6968
FM	3	0.00886	0.002955	F _{critical} = 9.55
RM	5	0.01889	0.003779	df = (2, 3)
<i>Shape factor (Y₂)</i>				
Regression				
FM	5	0.03882	0.007765	0.9974
RM	4	0.038807	0.009702	0.9970
Residual				F _{cal} = 0.4892
FM	3	9.8E–05	3.27E–05	F _{critical} = 10.13
RM	4	0.000114	2.85E–05	df = (1, 3)
<i>Carr's index (Y₃)</i>				
Regression				
FM	5	17.48569	3.497138	0.9697
RM	4	17.41047	5.803489	0.9655
Residual				F _{cal} = 0.2067
FM	3	0.545708	0.181903	F _{critical} = 10.13
RM	5	0.620933	0.124187	df = (1, 3)

^a FM, Full model.
^b RM, Reduced model.
^c df, Degree of freedom.
^d SS, Sum of squares.
^e MS, Mean of squares.

2008.6.03 (Addinsoft, Italy). The scree plot shown in Fig. 6 shows the eigenvalues for each component in descending order. The aim was to look for a “large gap” or an “elbow” in the graph. The rate of decline tends to be fast first then levels off. The ‘elbow’, or the point at which the curve bends (dotted line in Fig. 6), was considered to indicate the maximum number of PC to extract. This scree plot revealed that there was one large gap/break in the data between components 1 and 2 and then the eigenvalues begin to flatten out beginning with component 3. This indicated that only these two components (1 and 2) should be retained and interpreted. A sequential analysis would likely show that components 3 to 9 appeared after the break was assumed to be trivial and hence not retained. Also eigenvalues of components 3 to 9 were less than unity (1) and can therefore be removed and not interpreted [58]. From the percentage cumulative variance plot (Fig. 6), it would appear to be 2 “dimensions” represented by components 1 and 2 which account for 90% of the variation in the data. At the end, it was speculated that the dg, SF and CI were the most important variables in the preparation of agglomerates of RL and, hence, further optimization of agglomerates was based on them.

4.2. Optimization of agglomerates

For all 9 batches, selected dependent variables mean geometric diameter (Y₁), shape factor (Y₂) and Carr's index (Y₃) exhibited wide variations from 0.497 to 1.075 mm, 0.788 to 0.978 and 14.27 to 19.24, respectively (Table 2). The data clearly indicated strong influence of selected factors (X₁ and X₂) on responses (Y₁, Y₂ and Y₃). The polynomial terms could be used to draw conclusions after considering the magnitude of coefficients and mathematical sign it expresses either positive or negative (Table 3) which are graphically illustrated in Fig. 7.

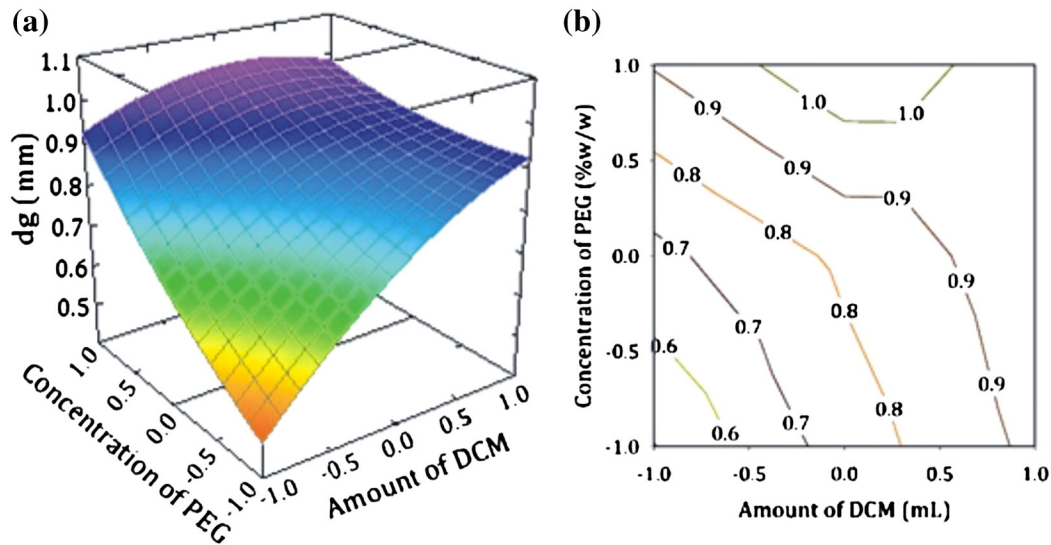


Fig. 8. Influence of formulation variable amount of DCM (X_1) and concentration of PEG (X_2) on dg (Y_1) by (a) response surface and (b) counter plot.

Using 5% significance level, a model was considered significant if the P-value (significance probability value) was less than 0.05. For dg (Y_1), coefficients b_{11} and b_{22} were found to be insignificant ($P > 0.05$) and therefore, these terms were separated from their full model in order to develop reduced model (Table 3). Similarly, the coefficient b_{12} was insignificant for SF (Y_2) and b_{22} along with b_{12} were found to be insignificant for CI (Y_3) and hence, these terms were removed from their respective full model [22]. The removal of insignificant terms was further justified by executing ANOVA test (Table 4). The high values of correlation coefficients for dg (Y_1), SF (Y_2) and CI (Y_3), illustrated goodness of fit [59]. The critical values of F for Y_1 , Y_2 and Y_3 were found to be 9.55 (df = 2, 3), 10.13 (df = 1, 3) and 10.13 (df = 1, 3), respectively. For all responses, calculated F values [1.69 (Y_1), 0.48 (Y_2) and 0.21 (Y_3)] were less than their respective critical values which advocated nonsignificant difference amongst full and reduced model [60,61]. The data of all 9 batches of experimental design were used to generate interpolated values with the assistance of contour and perturbation plots [62].

4.2.1. Influence of formulation composition on mean geometric diameter (Y_1)

The results of regression analysis for dg (Y_1) depicted positive sign for regression coefficients b_1 and b_2 which suggested that with an increase in amount of DCM (X_1) and concentration of PEG (X_2) the dg of RL agglomerates resulted in an increased. A highest dg of 1.075 was observed for batch RL8 with levels of X_1 and X_2 as 0 and 1, respectively. The results of response surface and contour plots are illustrated in Fig. 8. From the response surface and contour plot it was clear that dg of RL agglomerates was increased with increased amount of DCM and PEG concentration. This could be attributed to the presence of higher amount of DCM which might had provided good bonding of crystals and ultimately increased size [14]. Additionally, an increase in size of agglomerates with increased PEG concentration might be attributed to the ability of PEG to bind the growing crystals during crystallization.

As the number of response surface methodology (RSM) factors increased, it became difficult to visualize the response surface with graphical tools. In this case it is helpful to view a special form of

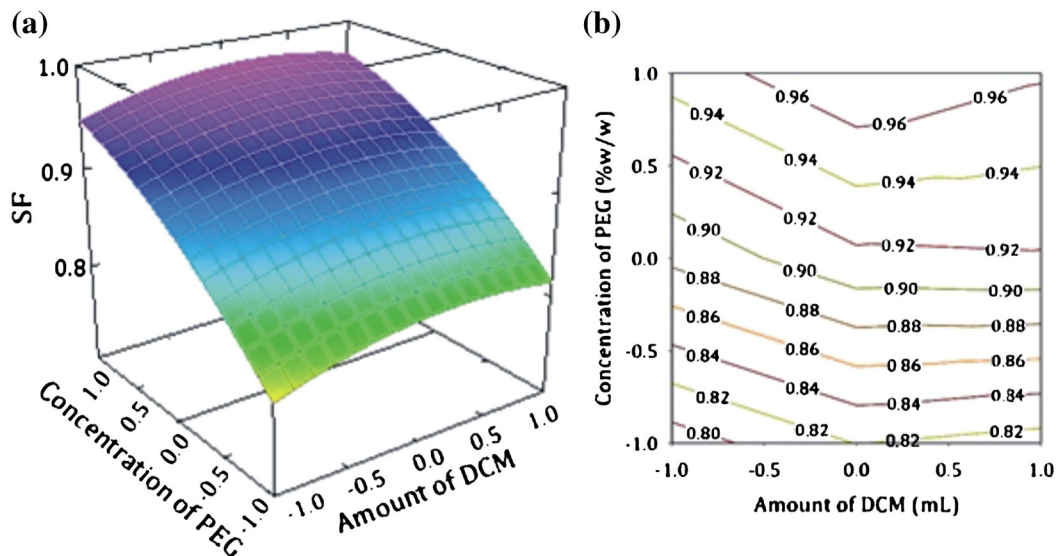


Fig. 9. Influence of formulation variables on SF (Y_2) by (a) response surface and (b) counter plot.

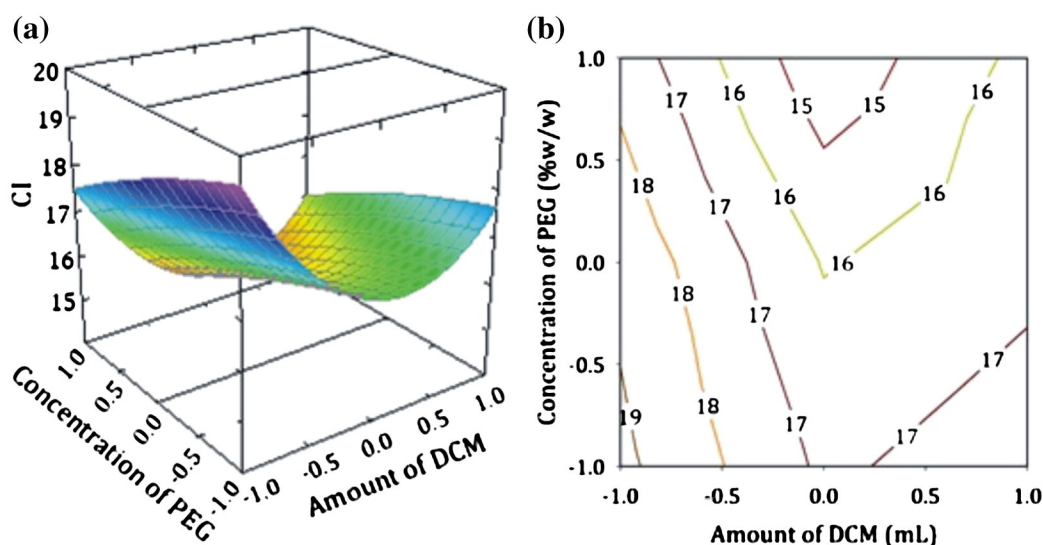


Fig. 10. Influence of formulation variables on CI (Y_3) by (a) response surface and (b) counter plot.

response plot called “perturbation” for RSM data. Perturbation plots compared the effect of all the factors at a particular point in the RSM design space. The response was plotted by changing only one factor over its range, while holding all other factors constant. On the perturbation plot, a steep slope or curvature in an input variable indicates a relatively high sensitivity of response. Perturbation plot in Fig. 8a illustrated the effect of X_1 and X_2 variables on the dg. Increase in dg was observed as the amount of DCM and concentration of PEG increased with same magnitude. Again this observation was also confirmed by surface response and counter plot (Fig. 9) along with regression analysis (Table 3 and Fig. 7a).

4.2.2. Influence of formulation composition factor on shape factor (Y_2)

The results of regression analysis for Y_2 depicted positive sign for regression coefficients b_1 and b_2 . This finding suggested that shape factor (SF) of RL agglomerates was increased as X_1 and X_2 increased. A highest SF of 0.978 was observed in batch RL8 with levels of X_1 and X_2 as 0 and 1, respectively. The results of response surface and contour plots are illustrated in Fig. 10. This finding also correlated with the observation of perturbation plot (Fig. 8b). In addition to these, high magnitude of regression coefficient b_2 (0.0778) indicated PEG had more positive influence on the sphericity of RCD agglomerates as compared to DCM (Table 3). PEG was the crucial polymer which could alter the crystal habit and the manner in which drug got recrystallized by giving a spherical shape. This might be attributed to adsorption of PEG at the growing surface of agglomerates and controlling or blocking the rate/growth of crystal formation [63,64].

4.2.3. Influence of formulation composition factor on Carr's index (Y_3)

The results of regression analysis for Y_3 described negative sign for regression coefficients b_1 and b_2 (Table 3). This suggested that with increased in amount of DCM and concentration of PEG the CI of agglomerates was decreased. These results are observed in response surface and contour plots (Fig. 11). Perturbation plot (Fig. 8c) depicted that X_1 influence strongly on CI which was confirmed by high magnitude of regression coefficient b_1 (-0.836). The curve corresponding to X_1 declines from -1 to 0 and then rises gradually up to level 1 . This finding revealed that at low level of DCM, the CI decreased and at last the flowability of agglomerates was improved. Further, the sphericity of prepared agglomerates reduced at higher amount of DCM which might be due to the roughness imparted by DCM on growing agglomerates. The lower magnitude of regression analysis for X_2 showed the

lesser impact on CI and it was confirmed from perturbation plot (Fig. 8c).

The optimized formulation was obtained by applying constraints on dependent variable responses and independent variables [65]. The constraints were arbitrarily selected as dg in range of 0.5 to 1 (mm); SF target to 1 and minimum CI. These constraints were common for all the formulations. The recommended concentrations of the independent variables were calculated by the Design Expert® version 7.1.5 (Stat-Ease, Inc., MN, USA) software from the overlay plot (Fig. 12). The optimum values of selected variables obtained were 0.22 (X_1) and 0.86 (X_2). Check point/optimized batch of RL agglomerates (RLO) comprised 7.66 mL of DCM, 4.79% w/w of PEG, 1% w/w of talc and 2% w/w of PVA with a stirring rate of 875 rpm. The results depicted nonsignificant ($P > 0.05$) difference and lower magnitude of % relative error between experimentally obtained and theoretically computed data of dg, SF and CI [23] along with significant values of R^2 [66] suggested the robustness of mathematical model and high predictive ability of full factorial design applied (Table 5).

4.3. Percentage yield and drug content

Almost all the batches of agglomeration showed drug content $>96\%$. The results indicated good loading efficiency and insignificant drug loss which might be attributed to slight solubility of RCD in poor solvent and addition of LPM to poor solvent. The % yield of prepared agglomerates is shown in Table 2. The percentage yield of agglomerated crystals was found in the range of 89.35% to 97.32%. The variation in % yield might be attributed to drug loss during agglomeration in terms of sticking to the wall of the vessel and remaining unagglomerated.

4.4. Shape analysis

Aspect ratio (ϕ), shape factor (SF) and circularity factor (CF) for prepared agglomerates were varied between 0 and 1, with a low value which indicated an elongated particle; a perfect sphere had an aspect ratio of 1. As seen in Table 2, the values of these descriptors are near to unity. Irregularity gave an indication of whether or not the particle was elongated or irregular. Irregularity measures the surface area compared to the size of the particle, a perfect circle has an irregularity of π . The low value of IF of RL crystals (1.982) was gave an indication of elongated particle shape. The value of IF of optimized RL agglomerates was found to be 3.016 which indicated perfect spherical structure of agglomerates and it was confirmed from SEM. Elongated or irregular

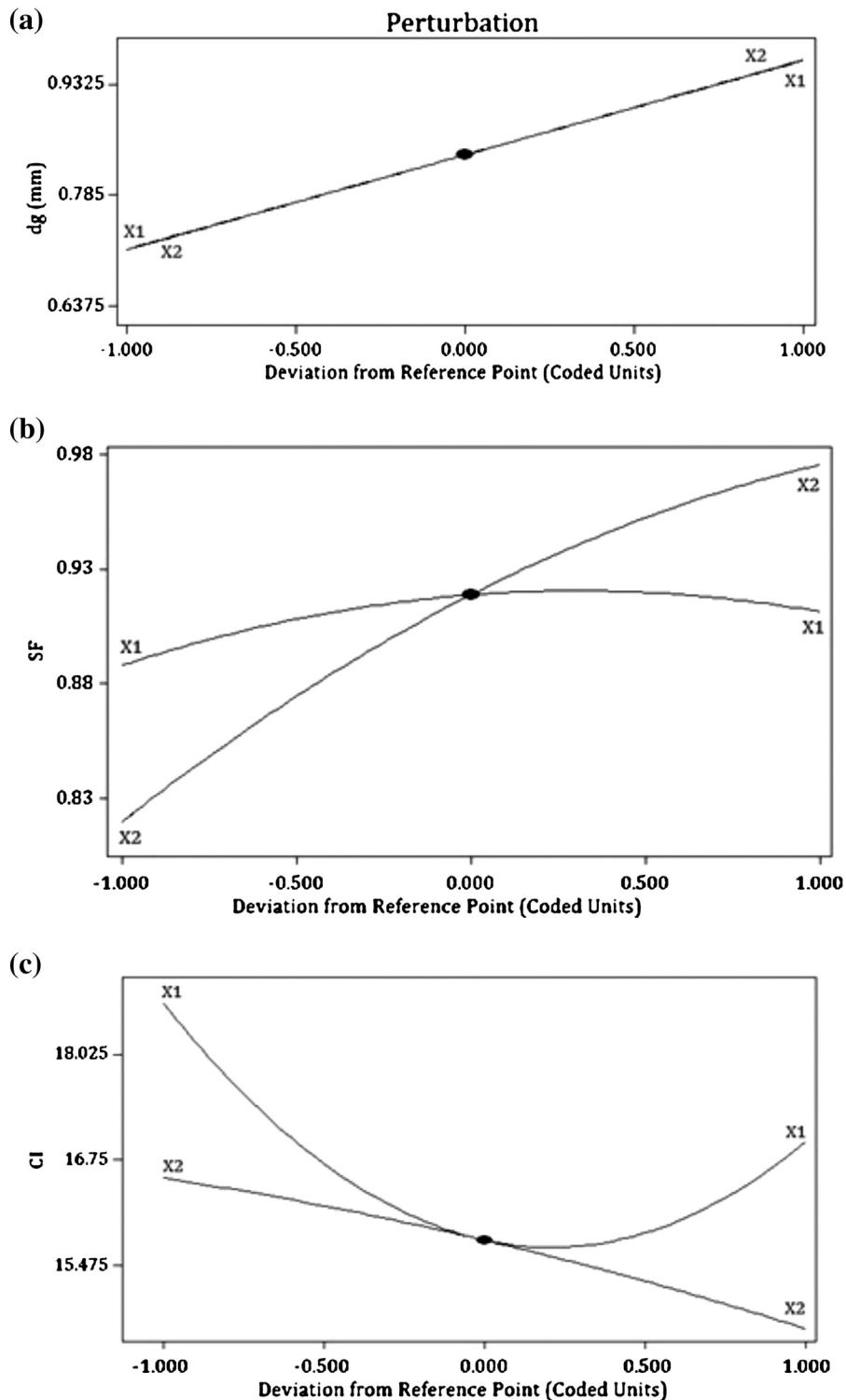


Fig. 11. Perturbation plots showing effect of independent factors on (a) dg, (b) SF and (c) CI of agglomerates while keeping other variables at their respective midpoint.

particles might tend to mechanically interlock or entangle with each other, thus obstructing powder flow and reducing flowability [67]. Considering the shape parameters in combination can give more detailed information. For instance, prepared RL agglomerates by CCA were more spherical in shape whereas RCD and LPM crystals were elongated and irregular in silhouette. The majority of drugs do not present adequate flow properties and high compressibility necessary for direct compression, requiring addition of excipients, which strengthens the weak linking between particles, facilitating the cohesion of the materials and, consequently, the compression [68].

4.5. Flowability measurements

The widespread use of solids in industries related with agricultural, food, chemical, ceramic, pharmaceutical, metallurgical, and other bulk solids and powder processing has generated a variety of techniques for characterizing flow behavior of solids. Improved processability refers to any advancement, which would enable downstream dosage form development or packaging, such as enhanced flowability and compressibility. Flow is well-defined as the relative movement of a bulk of particles among neighboring particles, or along the wall surface

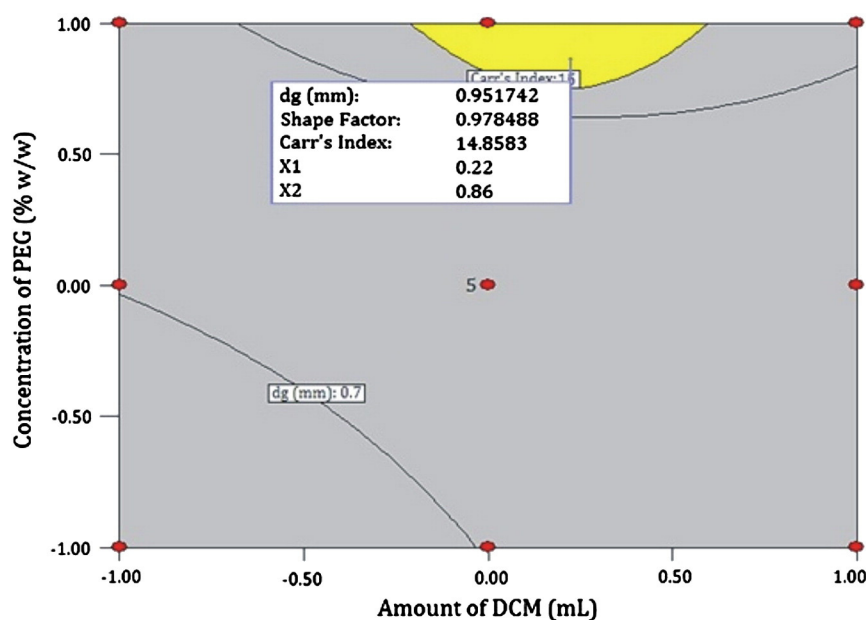


Fig. 12. Overlay plot for optimized parameters of agglomerates.

of a container. Poor flow properties affect adversely the ability to process such materials, for example, by hindering the mixing process and potentially affecting process performance. To ensure steady and reliable flow, it is crucial to accurately characterize the flow behavior of solid materials.

As shown in Table 2, flow property of agglomerates obtained in the presence of excipients was excellent compared to RCD and LPM. Remarkable reduction in CI and HR as well as AoR of agglomerates compared to physical mixture of pure drugs indicated substantial improvement in flow and packing ability of agglomerates. This was due to spherical shape and smooth surface of the agglomerates obtained from the process of agglomeration.

4.6. Compression behavior of coarse and agglomerated RL

An important approach in practice is the focus on the manufacturing of tablets with adequate strength. This ability of a powder or agglomerate formulation to be compressed into tablets with specified strength can be expressed as the formulations' compactibility or packability. Attempts have been made to describe the entire compression profile in distinct parts by several equations [69] or with a polynomial with several coefficients [70]. In order to investigate compression behavior of prepared agglomerates, Kawakita analysis, Kuno's equation and Heckel analysis were performed.

Kawakita parameters were obtained by linear regression analysis (Fig. 13). The linear region of the Kawakita plot was determined visually, and for all the plots was taken between 0 and 100 tapping.

Table 5
Results of optimized batch (RLO) of agglomerates.

Response	Predicted value	Experimental value [Mean ± SD (n = 3)]	% Relative error
dg (mm)	0.9517	0.9015 ± 0.1205	5.27
SF	0.9784	0.9641 ± 0.1132	1.46
CI	14.8583	15.3826 ± 0.0971	3.52

The R^2 values for both RL and all other batches including RLO (indicated by line graph in Fig. 13) were >0.9 . The parameter a explains the initial porosity at zero pressure which is corresponding to the total portion of reducible volume at maximum pressure. It also describes the relative volume reduction at the maximum number of taps. In case of prepared agglomerates of RL, the value of a (<0.157) was significantly smaller than value of RL (0.416), indicating excellent flowability and better packability of agglomerated crystals over RL. Here, RL had higher a value than RLO which could be attributed to needle shape structure of primary RL particles, possessing large amount of voids between them. Smaller a value of RLO was due to the smaller size and spherical shape of the particles, which would facilitate efficient packing [71]. In other words they were well packed before tapping since tapping does not improve the packing significantly, it only reorganizes the agglomerated particles presumably without changing their shape and size significantly [72]. The apparent packing velocity obtained by tapping, represented by parameter $1/b$, for the agglomerates was lower than that for the pure drug, since the agglomerates were packed more closely, even without any tapping, as a consequence of their better flowability and packability [73]. Mathematically the parameter $1/b$ is equal to the pressure when the value of C reaches one-half of the limiting value, and for the prepared agglomerates the $1/b$ parameter range from 2.806 to 8.854. The $1/b$ values for RL and RLO were 16.845 and 3.472 respectively. Thus, RLO requires greater force to reduce to one half of its original volume than RL, as needle shape crystals get packed with high amount of rearrangement, which requires higher force. The larger b value of RLO

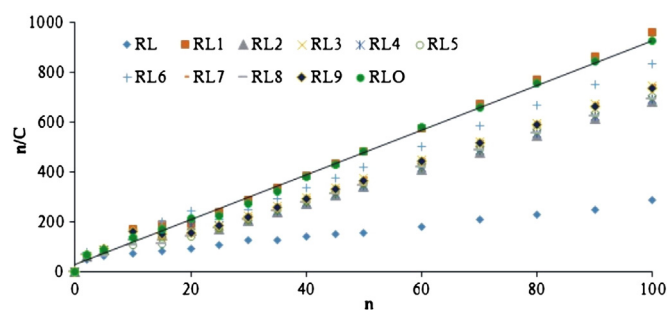


Fig. 13. Kawakita plot of pristine drugs and agglomerates.

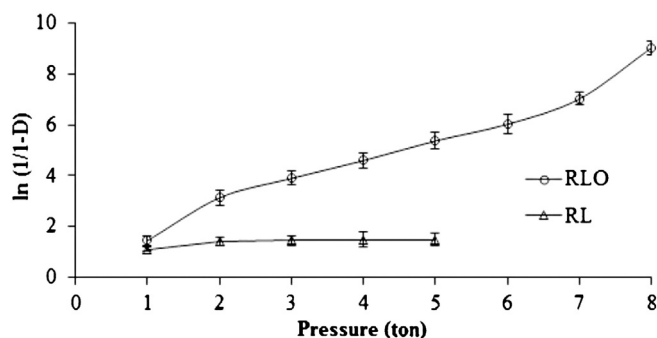


Fig. 14. Heckel plot of pristine drugs and optimized agglomerates.

(0.288) than RL (0.0593) implied that comparatively less resisting forces could occur for agglomerated crystals during compression [74]. Improved flow properties and compressibility of the agglomerated crystals indicated that they were directly compressible; whereas, the non-agglomerated drug would be predicted to be not directly compressible due to its poor flow properties. In mechanistical terms, the powders became more resistant to compression at the lower pressure range opposite to agglomerates. The compression profiles also indicated that smaller particle size of drug tended to reduce the ability of the powders to compress. This may reflect that smaller size materials resulted in less prone to deform.

Furthermore, large values of parameter K (>0.9) in Kuno's equation for the agglomerates indicated that the rate of their packing process was much higher than that of the original crystals. These findings suggested that agglomerates flow and pack smoothly from the hopper into the die and that tablets formed from agglomerates attain uniformity in weight [73,75].

The Heckel equation is probably the most widely used porosity-pressure function in the field of pharmaceutical sciences. Heckel suggests [35] density-pressure relationship during powder compaction in analogous to a first order chemical reaction. Heckel plot constant, A is the intercept of the extrapolated linear region of the curve (Fig. 14). Its value is related to the density of the powder after die filling and particle rearrangement in the initial phase of compaction before bond formation. Values of A for all batches of agglomeration were less than pure drugs (1.128). This finding suggested that, low compression pressure was required to obtain the closest packing of the particle, fracturing its texture and densifying the fractured particles [76]. Heckel [34] argued that the linear part of the curve described the plastic deformation of the material and considered elastic deformation to be negligible. The slope of the linear region of the curve, k , provided information of the plasticity of the compressed powder. The higher the value of the slope k for all prepared batches indicated the more plastic nature of agglomerates than the RL. The value of slope was also related to the mean yield pressure (P_y) of the material [77], which measured the material's resistance for deformation. Plastic flow of the particles during

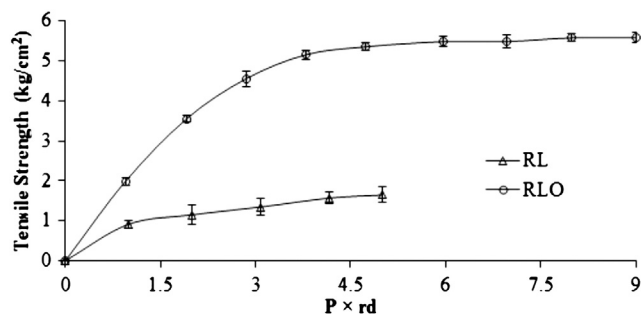


Fig. 15. Leuenberger plot of pristine drugs and optimized agglomerates.

Table 6
Parameters of Leuenberger equation.^a

Sample	Compression susceptibility, γ (kg/cm ²) ⁻¹	Maximum crushing strength, σ_{tmax} (kg/cm ²)
RL	0.0211 ± 0.0089	1.645 ± 0.197
RLO	0.0937 ± 0.0115	5.578 ± 0.128

^a Results are of mean of three observations ± SD.

compression occurred mainly after rearrangement and fracture [78]. The Heckel yield pressure, P_y , represented the compressibility of the powder in region II, varied from 28.43 tons (RL) to 1.271 tons (RL1), i.e. a ~ 22-fold variation. Since, the Heckel yield pressure is often used as an indication of the plasticity of materials, the agglomerates prepared represented that was soft and RL considered as hard, as categorized by Roberts and Rowe [79].

Yield strength (σ_o) is an indication of the tendency of the materials to deform either by plastic flow or fragmentation [80]. The low value of yield strength (σ_o) (Table 2) was again an indication of low resistance to pressure, good densification and easy compaction [75]. Heckel also concluded that at low pressures the curved region of the plot was associated with individual particle movement in the absence of interparticle bonding, and that the transition from curved to linear corresponds with the minimum pressure necessary to form a coherent compact [35]. In case of agglomerates, the effect of PEG addition (plastic material) on tableting properties was observed. Densification of this polymer was probably due to plastic deformation [81]. Furthermore, Heckel plot analysis suggested that, agglomerated crystals were fractured easily and new surface of crystals produced might contributed to promote plastic deformation under compression [82]. Therefore, it was concluded that compressibility and tableting behavior of RL was successfully improved by CCA technique. Furthermore, compressibility of optimized agglomerated RL was determined by using 4.7 Leuenberger analysis.

Leuenberger derived an equation, which includes one factor for the compressibility and one for the compactibility [83]. The inclusion of a compactibility term made this equation, the so-called Leuenberger equation, an attractive tool for investigating powder formulations. Interrelation between these two characteristics can be expressed with following equation.

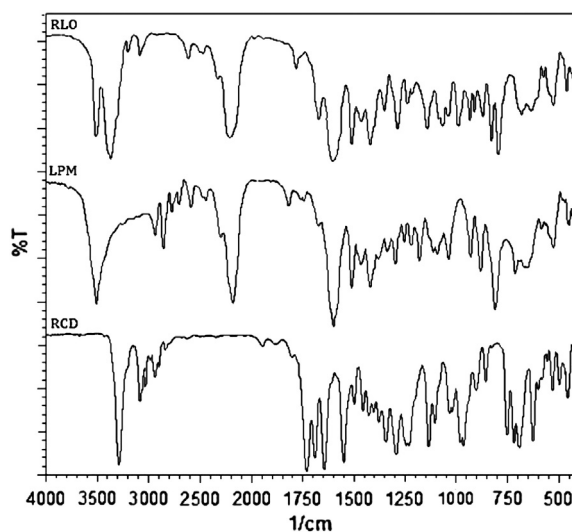


Fig. 16. FT-IR spectra of RCD, LPM and RLO.

$$\sigma_t = \sigma_{tmax} (1 - e^{-\gamma P \rho}) \quad (16)$$

where σ_t is the radial crushing strength at certain pressure (kg/cm^2); σ_{tmax} is the maximum crushing strength (MPa); γ is compression susceptibility ($(\text{kg}/\text{cm}^2)^{-1}$); P is the applied force and ρ is the relative density. A nonlinear plot (Fig. 15) of tensile strength with respect to product of compaction pressure (P) and relative density (ρ) was obtained using statistical software GraphPad Prism 5.03 (GraphPad Software, Inc. USA). The parameter maximum crushing strength (σ_{tmax}) and compression susceptibility (γ) allow a characterization of the different materials [84]. The compression susceptibility for compact prepared from RLO indicated that the maximum crushing strength was reached faster at lower pressures of compression as opposed to crystals of RL. Higher value for σ_{tmax} was observed in case of agglomerates than coarse RL compression. It showed that agglomerates can build a compact with a higher strength than RL. The lower value of γ for RL crystals demonstrated that maximum tensile strength could be obtained slowly at higher pressure. The low σ_{tmax} value for powder showed poor bonding properties which indicated least bonding properties of compact prepared from coarse RL crystals (Table 6).

4.7. Elastic recovery

To investigate the effects of interparticulate friction, elastic recovery measurements were made on prepared compacts. The result of elastic recovery for RL and agglomerates are given in Table 2. Elastic recovery of all prepared agglomerates was very small ($<0.82\%$). Capping/lamination of the original coarse crystals occurred at compression pressures of 4 tons and above. At the same time, the elastic recovery of pure drugs was very high (4.43%). When RL was made into agglomerates by CCA, tableting was possible without the occurrence of capping. Spherically agglomerated crystals of RL was significantly better tabletability than coarse crystals, because agglomerates making the crystals fracture easily under compression, this increased the points of contact among particles facilitated plastic flow, thereby increasing the contact area and new high-energy surfaces appeared because of fracturing, which strongly bonded the particles [82,85].

4.8. Tensile strength

The agglomerated crystals, obtained by crystallization in the presence of excipients like HPMC and PEG, possessed superior tensile

strength characteristics in comparison to the pure crystals (Table 2). The results showed that the tablets made of untreated RL particles were prone to capping at lower compression pressures. Whereas, the agglomerated crystals were successfully tableted without capping at any compression pressure applied. This was the main reason for higher tensile strength of tablets made from agglomerated particles in comparison with the tablets made from the untreated RL ($1.645 \text{ kg}/\text{cm}^2$). The maximum tensile strength for RLO ($5.578 \text{ kg}/\text{cm}^2$) was obtained at compression pressure 9 tons.

4.9. Moisture content

The moisture content of a pure drugs and agglomerates influenced flowability from the perspective of capillary forces and liquid bridging between the particles. The strength of the cohesive force depends on the surface tension, wetting angle, space between the particles and particle diameter. The same particle characteristics that result in moisture uptake would influence dissolution properties. This parameter was also important for the prediction of the flow behavior of the product in the tableting machines or in the encapsulation machines during the preparation of pharmaceutical dosage forms. It is worthwhile to note that moisture played a critical role in compression. One of the most common causes of capping in tablets was inadequate moisture in the blend ready for compression. In terms of residual moisture, results of moisture content of the agglomerated crystals of RL were found to be less than 1.3% (Table 2), which could be attributed to the hygroscopic nature of PEG that retained moisture, even after drying [86]. The data were in compliance with USP requirements for product storage [87].

4.10. Fourier transformed infrared (FT-IR) spectroscopy

Infrared (IR) spectral measurements have been used for a broad range of applications – from analysis of liquids, gas compositions and solid substances for detailed characterization of their physical state. The compatibility of RCD and LPM with polymers was investigated by IR spectroscopy study and the IR spectra of pure RCD, LPM and RLO are illustrated in Fig. 16. One of the fundamental properties of chemical bonds is that they exhibit vibrations at distinct frequencies. The vibrational frequency of a chemical bond is intrinsic to the

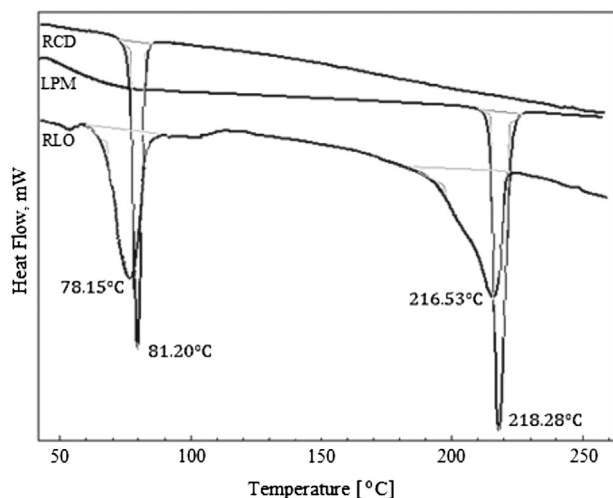


Fig. 17. DSC thermogram of RCD, LPM and RLO.

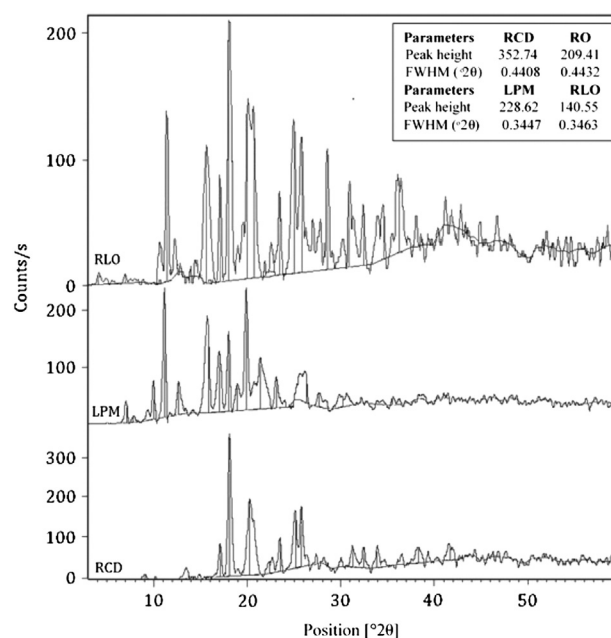


Fig. 18. PXRD patterns of RCD, LPM and RLO.

chemical bond of interest [88]. The study of IR spectra of RCD (Fig. 16) demonstrated characteristic absorption bands for aromatic rings like S–H stretching, C=O stretching, C–O stretching and N–H stretching vibration appeared at 1542, 2554, 1641, 1039 and 3306 cm^{-1} , respectively. Furthermore, IR spectra of LPM (Fig. 16) revealed that the characteristic absorption bands of C=O stretching, CH_2 stretching and O–H stretching vibration appeared at 1603, 2854 and 3562 cm^{-1} , respectively. Almost identical absorption bands were obtained from FT-IR spectra of optimized agglomerates (RLO), but with somewhat lower intensity. Thus, the IR study indicated a stable nature of RCD and LPM in agglomerates prepared by CCA. All the peaks of drugs appeared in the spherical agglomerates of RL, which showed that there was no any interaction between drug and excipients utilized.

4.11. Differential scanning calorimetry (DSC)

The DSC thermograms of RCD, LPM and RLO have been demonstrated in Fig. 17. Pure RCD and LPM showed a sharp endothermic peak at 81.20 °C and 218.28 °C, with the heat of fusion/enthalpy (ΔH) of 71.3 J/g and 76.31 J/g, respectively corresponding to melting points. These sharp peaks confirmed the purity of the drug substances, with no noticeable impurities present, corresponding to the literature value of 80.9 °C and 218.4 °C for RCD and LPM respectively [89,90]. In DSC thermogram of RLO, two endothermic peaks correspond to RCD and LPM at 78.15 °C and 216.53 °C respectively with a reduction in ΔH of RCD (44.81 J/g) and LPM (52.14 J/g). These occurrences might be attributed to the dispersion of crystalline RCD and LPM into amorphous polymers i.e. PEG and HPMC. Furthermore, it was not a sign of pharmaceutical incompatibility [91,92]. Partial amorphization of crystalline RCD and LPM in agglomerates might also be a reason for such phenomena [93]. Literature revealed that complete amorphous form of drugs was not in the equilibrium state and might be recrystallized during storage, granulation or compression processing [94]. Therefore, partial amorphization of RCD and LPM might be provided comparative more stability than their complete amorphous counterparts. In order to evaluate the amorphous/crystalline property quantitatively, the relative ratio of heat of fusion against the original bulk, was defined as crystallinity (X_{cr}), and it was calculated from the heat of fusion of DSC thermogram. The X_{cr} of RCD and LPM in RLO was found to be 0.6285 and 0.6833, respectively which were significantly smaller than pure crystalline drugs.

4.12. Powder X-ray diffraction (PXRD)

PXRD can be used to screen for the relative crystallinity of samples [95] which is expressed in terms of relative degree of crystallinity (RDC) or crystallinity index [96]. For the determination of the degree

of crystallinity, numbers of X-ray diffraction methods were reported and practiced [97]. Typically PXRD assessed crystallinity from peak height [98] or area [99]. In the present investigation, RDC was calculated by the following equation:

$$\text{RDC} = I_s/I_r \quad (17)$$

where, I_s was the peak height of the sample (optimized agglomerated crystals) under investigation and I_r was the peak height at the same angle of the reference (crystalline drug) with the highest intensity. Because crystalline drug was not observed “halo” in the PXRD pattern, the external standard method was reduced to a direct comparison method and therefore, it was assumed that coarse crystalline drugs had 100% crystallinity. Similarly, the relative crystallinity (RC) in percentage was calculated as follows:

$$\text{RC} (\%) = (C_s/C_r) \times 100 \quad (18)$$

where, C_s and C_r were the product of peak height and Kubler Index (is the full width at half-maximum height, FWHM) [100] of highest intense peak of sample (optimized agglomerated crystals) and reference (crystalline drug), at same angular scale, respectively.

The PXRD pattern of RCD and LPM exhibited intense peaks whereas PXRD pattern of agglomerated crystals (RLO) exhibited less intense and denser peaks compared to pristine RCD and LPM (Fig. 18). The PXRD pattern of RCD showed its characteristic peaks at 2θ of 18.04, 20.22, 25.69, 25.13, 23.56, 17.10, 41.71 and 31.34. Moreover, PXRD spectra of LPM exhibit clear diffraction peaks at 2θ of 11.6, 16.7, 17.5 and 20.2. In case of RLO, PXRD pattern in the 2θ range of 5 to 50 illustrated characteristic diffraction peaks of RCD and LPM. Intensities of characteristic peaks of drugs were decreased in RLO, which might be due to the differences in the crystallinity of the drugs and agglomerates [101], and indicated reduction in crystallinity or partial amorphization of the drugs in its agglomerated form [102]. In relative crystallinity determinations, the PXRD patterns of RCD and LPM were clearly different in peak intensity from corresponding peaks in RLO. The calculated RDC value of RCD and LPM in agglomerates (RLO) was 0.59 and 0.62 respectively which further indicated the reduction in crystallinity of drugs when formulated as spherical crystal agglomerates. Further, calculated RC values of RCD and LPM in optimized agglomerates were 59.69% and 61.76% respectively. In addition to these, it was found that the particles crystallized in the presence of excipients did not undergo structural modifications. As depicted in Fig. 18, most of PXRD peaks of the agglomerates were consistent with the pattern of pure drugs, which indicated that there was no any structural change or drug-excipients incompatibility detected after recrystallization [103].

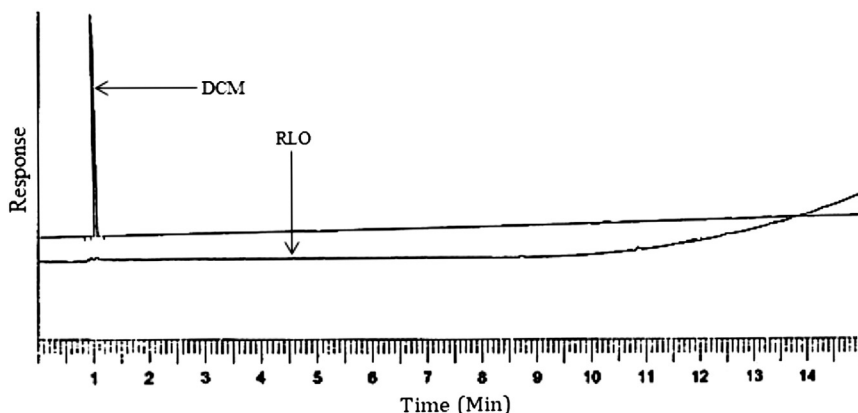


Fig. 19. GC-MS chromatogram for the determination of DCM in agglomerates.

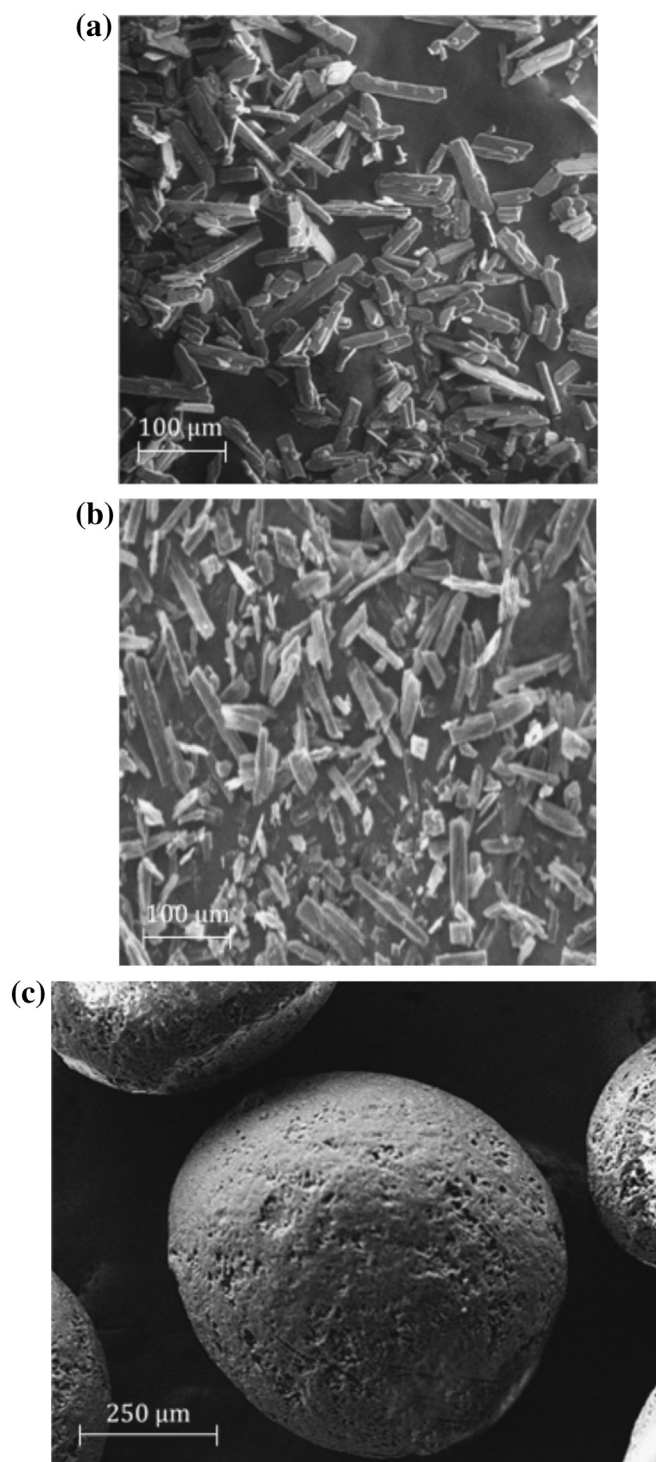


Fig. 20. SEM micrographs of (a) coarse RCD, (b) coarse LPM and (c) optimized agglomerates.

4.13. Determination of residual solvent

Residual solvents are critical impurities in excipients, drug substances and ultimately drug products, because they may cause toxicity and safety issues, and affect physicochemical properties of drug substances and drug products [104]. In order to control residual solvent contents in drug substances, products and excipients, ICH Q3C guideline provided particular criteria for Class 1 solvents (5) – known or suspected human carcinogens or environmental hazards, Class 2

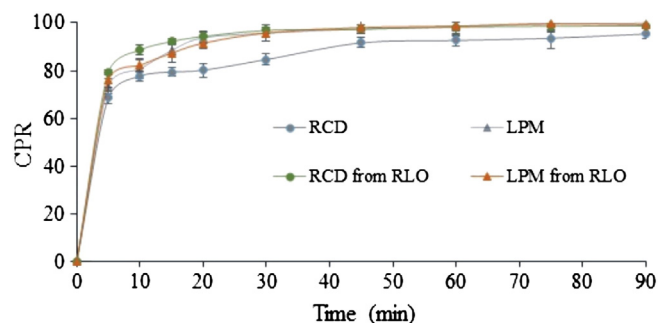


Fig. 21. Dissolution profile of RCD and LPM from optimized agglomerates (RLO).

solvents (26) – suspected of other significant but reversible toxicities, and Class 3 (28) solvents – low toxic potential to human [105]. Generally, the solvents were not completely eliminated by manufacturing techniques. Hence, the solvent might sometimes be a critical parameter in the process. The general procedure of European Pharmacopoeia for residual solvents determination in pharmaceutical products included analysis of many solvents by GC [106].

A GC-HS chromatogram of standard solution and agglomerates is shown in Fig. 19. The detector voltage (y-axis) was plotted as a function of time (x-axis). The identity of each peak can be determined by injecting samples and noting their retention times. After injecting standard solution of DCM (1000 ppm), a peak corresponding to a DCM content appeared at retention time of 1.03 min. A residual solvent peak of optimized RL agglomerates was observed at same retention time as that of standard (1.03 min) with extremely low intensity. It depicted that most of the solvents were evaporated and very small amount of solvent retained in agglomerates. Furthermore, the amount of DCM was determined by the area covered by peak at same retention time and it was found that 17.75 ppm. The “permitted daily exposure” (PDE) for DCM was defined by ICH as 600 ppm [105], it revealed that DCM was entrapped in agglomerates at insignificant extent and that it does not produce toxicity in human.

4.14. Scanning electron microscopy

An examination of the SEM, confirmed that the pristine RCD (Fig. 20a) and LPM (Fig. 20b) was significantly smaller in particle size and blade or plate shaped elongated crystals with fines which hindered the flowability and compressibility. Improved flowability of RL agglomerates was mainly because of good sphericity of modified crystals obtained (Fig. 20c) by CCA. Similar results were obtained in other studies using CCA procedures for other drugs [19,33,107]. SEM of the untreated RCD and LPM revealed no evidence of porosity in the untreated crystals whereas the agglomerated drugs indicated clear evidence of porosity. RCD and LPM crystallized and agglomerated in the presence of HPMC and PEG (Fig. 20c) were spherical in shape along with smooth surface appearance which promotes the flowability.

4.15. In vitro dissolution study

Dissolution of optimized agglomerates (RLO) and pure drugs (RCD and LPM) in optimized media was performed using USP type II apparatus [108]. The aliquots of dissolution were subjected to analysis by HPLC method. Dissolution profile of optimized agglomerates (RLO) showed 98.77% of RCD and 99.24% of LPM release within 90 min whereas pure RCD and LPM showed initially slower dissolution rate (Fig. 21). The reason for this improved dissolution was linked to the better wettability of the spherically agglomerated crystals. Incorporating the hydrophilic polymer might contribute in the improvement

of dissolution rate. The increase of the dissolution rates of drugs from agglomerates was also attributed to the reduction in crystallinity [109].

5. Conclusions

It was shown that QbD approach can be successfully used in the development of agglomerates containing RCD and LPM with predictable physico-chemical properties. It was demonstrated that multivariate methods, such as full factorial experimental design, response surface modeling, optimization and PCA, can be applied to systematically characterize the root-cause or source of variability. Crystallo-coagglomeration technique can be successfully employed as an alternative to conventional wet granulation. This study showed that it is possible to quantify differences between pristine RCD and LPM crystals and agglomerated RL by a quick and simple screening method. The RL agglomerates were successfully prepared by application of full factorial experimental design and characterized by different 21 variables. In combination with multivariate evaluation methods such as PCA, this approach was successful in distinguishing, quantifying and predicting the most influencing variables of agglomerates. Based on these findings the present approach serves as the first step towards a 'formulation tool' for optimizing various agglomerate properties with respect to formulate directly compressible tablet. In addition these RL agglomerates of RCD and LPM were obtained with excellent physico-mechanical properties. Agglomerates possessed increased particle size, sphericity and surface smoothness which resulted in excellent flow and packability due to reduced interparticulate friction. Optimized agglomerates consisting of 4.79% w/w of PEG, 1% w/w of talc and 2% w/w of PVA which were prepared at room temperature with god solvent (DCM) of 7.66 mL and stirring rate of 875 rpm. The dissolution study of the agglomerates showed slight increase in the rate of drug release compared to pure drugs. The systematic statistical approaches enable us to obtain ready-to-compress agglomerates of combined active pharmaceutical ingredients by omitting time consuming conventional wet granulation method using novel CCA technique. It can be concluded that multivariate methods, as QbD principles and tools, play an important role in simplifying a higher-level of process understanding and create opportunities for root-cause investigation and developing control strategies in pharmaceutical formulation and process development.

References

- [1] FDA Pharmaceutical Quality for the 21st Century a Risk-based Approach, Department of Health and Human Services, September 2004.
- [2] Y. Rouiller, T. Solacroup, V. Deparis, M. Barbaferi, R. Gleixner, H. Broly, A. Eon-Duval, Application of quality by design to the characterization of the cell culture process of an Fc-fusion protein, *European Journal of Pharmaceutics and Biopharmaceutics* 81 (2012) 426–437.
- [3] ICH, Guideline Q9: Quality Risk Management, Technical Report, Available from: http://www.ich.org/fileadmin/Public_Web_Site/ICH_Products/Guidelines/Quality/Q9/Step4/Q9_Guideline.pdf2005.
- [4] ICH, Guideline Q10: Pharmaceutical Quality System, Technical Report, Available from: http://www.ich.org/fileadmin/Public_Web_Site/ICH_Products/Guidelines/Quality/Q10/Step4/Q10_Guideline.pdf2008.
- [5] ICH, Guideline Q8R2: Pharmaceutical Development, Technical Report, Available from: http://www.ich.org/fileadmin/Public_Web_Site/ICH_Products/Guidelines/Quality/Q8_R1/Step4/Q8_R2_Guideline.pdf2009.
- [6] V. Lourenço, D. Lochmann, G. Reich, J. Menezes, T. Herdling, J. Schewitz, A quality by design study applied to an industrial pharmaceutical fluid bed granulation, *European Journal of Pharmaceutics and Biopharmaceutics* 81 (2012) 438–447.
- [7] I. Klevan, J. Nordström, I. Tho, G. Alderborn, A statistical approach to evaluate the potential use of compression parameters for classification of pharmaceutical powder materials, *European Journal of Pharmaceutics and Biopharmaceutics* 75 (2010) 425–435.
- [8] R. Roopwani, I.S. Buckner, Understanding deformation mechanisms during powder compaction using principal component analysis of compression data, *International Journal of Pharmaceutics* 418 (2011) 227–234.
- [9] S.T. Leonard, M. Droegge, The uses and benefits of cluster analysis in pharmacy research, *Research in Social & Administrative Pharmacy* 4 (2008) 1–11.
- [10] A. Johansen, T. Schaefer, H.G. Kristensen, Evaluation of melt agglomeration properties of polyethylene glycols using a mixer torque rheometer, *International Journal of Pharmaceutics* 183 (1999) 155–164.
- [11] S.R. Gokonda, G.A. Hileman, S.M. Upadrashta, Development of matrix controlled release beads by extrusion–spherization techniques technology using a statistical screening design, *Drug Development and Industrial Pharmacy* 20 (1994) 279–292.
- [12] A.R. Paradkar, M. Maheshwari, A.R. Ketkar, B. Chauhan, Preparation and evaluation of ibuprofen beads by melt solidification technique, *International Journal of Pharmaceutics* 255 (2003) 33–42.
- [13] O.L. Sprockel, M. Sen, P. Shivanand, W. Prapaitrakul, A melt extrusion process for manufacturing matrix drug delivery systems, *International Journal of Pharmaceutics* 155 (1997) 191–199.
- [14] Y. Kawashima, S.Y. Lin, M. Naito, H. Takenama, Direct agglomeration of sodium theophylline crystals produced by salting out in liquid, *Chemical & Pharmaceutical Bulletin* 30 (1982) 1837–1843.
- [15] S.S. Kadam, K.R. Mahadik, A.R. Paradkar, A process for making agglomerates for use as or in a drug delivery system. Indian Patent. 183036 (1997).
- [16] J.C. Schwartz, J.M. Lecomte, Form of administration of racecadotril. US Patent 20090186084A1 (2009).
- [17] M. Eberlin, T. Mück, M.C. Michel, A comprehensive review of the pharmacodynamics, pharmacokinetics, and clinical effects of the neutral endopeptidase inhibitor racecadotril, *Frontiers in Pharmacology* 3 (2012) 1–16.
- [18] K.C. Garala, A.J. Shinde, H.N. More, Solubility enhancement of aceclofenac using dendrimer, *Research Journal of Pharmaceutical Dosage Forms and Technology* 1 (2009) 94–96.
- [19] M.K. Raval, K.R. Sorathiya, N.P. Chauhan, J.M. Patel, R.K. Parikh, N.R. Sheth, Influence of polymers/excipients on development of agglomerated crystals of secnidazole by crystallo-co-agglomeration technique to improve processability, *Drug Development and Industrial Pharmacy* 39 (2013) 437–446.
- [20] K. Morishima, Y. Kawashima, H. Takeuchi, T. Niwa, T. Hino, Micromeritic characteristics and agglomeration mechanisms in the spherical crystallization of buccillamine by the spherical agglomeration and the emulsion solvent diffusion methods, *Powder Technology* 76 (1993) 57–64.
- [21] K.C. Garala, P.H. Shah, Influence of crosslinking agent on the release of drug from the matrix transdermal patches of HPMC/Eudragit RL 100 polymer blends, *Journal of Macromolecular Science, Part A* 47 (2010) 273–281.
- [22] B. Singh, M. Dahiya, V. Saharan, N. Ahuja, Optimizing drug delivery systems using systematic "design of experiments" Part II: retrospect and prospects, *Critical Reviews in Therapeutic Drug Carrier Systems* 22 (2005) 215–294.
- [23] B. Singh, R. Kumar, N. Ahuja, Optimizing drug delivery systems using systematic "design of experiments" Part I: fundamental aspects, *Critical Reviews in Therapeutic Drug Carrier Systems* 22 (2005) 27–105.
- [24] T.J. Shah, A.F. Amin, J.R. Parikh, R.H. Parikh, Process optimization and characterization of poloxamer solid dispersions of a poorly water-soluble drug, *AAPS PharmSciTech* 8 (2007) E1–E7.
- [25] G. Chaulang, K. Patil, D. Ghodke, S. Khan, Preparation and characterization of solid dispersion tablet of Furosemide with crospovidone, *Research Journal of Pharmacy and Technology* 1 (2008) 386–389.
- [26] A. Martin, J. Swarbrick, A. Cammarata, *Physical Pharmacy: Physical Chemical Principles in the Pharmaceutical Sciences*, Varghese Publishing House, Bombay, India, 1991.
- [27] N. Piipel, The flow properties of magnesia, *Journal of Pharmacy and Pharmacology* 16 (1964) 705–716.
- [28] R.L. Carr, Evaluating flow properties of solids, *Chemical Engineer* 72 (1965) 163–168.
- [29] H.H. Hausner, Friction conditions in a mass of metal powder, *International Journal of Powder Metallurgy* 3 (1967) 7–13.
- [30] K. Kawakita, Y. Tsutsumi, A comparison of equations for powder compression, *Bulletin of the Chemical Society of Japan* 39 (1966) 1364–1368.
- [31] H. Kuno, Funtai (Powder Theory and Application), in: K. Iino, J.K. Beddow, G. Jimbo (Eds.), Maruzen, Tokyo, 1979, p. 342.
- [32] S. Mallick, S.K. Pradhan, M. Chandran, M. Acharya, T. Digdarsini, R. Mohapatra, Study of particle rearrangement, compression behavior and dissolution properties after melt dispersion of ibuprofen, avicel and aerosil, *Results in Pharma Sciences* 1 (2011) 1–10.
- [33] N. Jadhav, A. Pawar, A. Paradkar, Design and evaluation of deformable talc agglomerates prepared by crystallo-coagglomeration technique for generating heterogeneous matrix, *AAPS PharmSciTech* 8 (2007) E1–E7.
- [34] R.W. Heckel, Density–pressure relationships in powder compaction, *Transactions of the Metallurgical Society of the American Institute of Mechanical Engineers* 221 (1961) 671–675.
- [35] R.W. Heckel, An analysis of powder compaction phenomena, *Transactions of the Metallurgical Society of the American Institute of Mechanical Engineers* 221 (1961) 1001–1008.
- [36] J.T. Fell, J.M. Newton, Determination of tablet strength by the diametral compression test, *Journal of Pharmaceutical Sciences* 59 (1970) 688–691.
- [37] N.A. Armstrong, R.R. Haines-Nutt, Elastic recovery and surface area changes in compacted powder systems, *Powder Technology* 9 (1974) 287–290.
- [38] P.J. Jaroz, E.L. Parrott, Comparison of granule strength and tablet tensile strength, *Journal of Pharmaceutical Sciences* 72 (1983) 530–535.
- [39] S. Srinivasan, B. Rengarajan, B. Prabagar, T. Pritam, S.Y. Chul, K.Y. Bong, Solid self-nanoemulsifying drug delivery system (S-SNEDDS) containing phosphatidylcholine for enhanced bioavailability of highly lipophilic bioactive carotenoid lutein, *European Journal of Pharmaceutical Sciences* 79 (2011) 250–257.
- [40] H.K. Jun, H.O. Dong, O. Yu-Kyoung, S.Y. Chul, C. Han-Gon, Effects of solid carriers on the crystalline properties, dissolution and bioavailability of flurbiprofen in solid

- self-nanoemulsifying drug delivery system (solid SNEDDS), *European Journal of Pharmaceutical Sciences* 80 (2012) 289–297.
- [41] S.P. Stodghill, Thermal analysis – a review of techniques and applications in the pharmaceutical sciences, *American Pharmaceutical Review* (April–March 2010) 29–36.
- [42] T. Niwa, Y. Nakanishi, K. Danjo, One-step preparation of pharmaceutical nanocrystals using ultra cryo-milling technique in liquid nitrogen, *European Journal of Pharmaceutical Sciences* 41 (2010) 78–85.
- [43] V.B. Cooper, G.E. Pearce, C.R. Petts, Quantification of crystalline forms in active pharmaceutical ingredient and tablets by X-ray powder diffraction, *Journal of Pharmacy and Pharmacology* 55 (2003) 1323–1329.
- [44] K. Esbensen, *Multivariate Analysis in Practice*, CAMO ASA, 2006.
- [45] K. Pearson, On lines and planes of closest fit to systems of points in space, *Philosophical Magazine Series* 6 (1901) 559–572.
- [46] T. Rajalahti, O.M. Kvalheim, Multivariate data analysis in pharmaceuticals: a tutorial review, *International Journal of Pharmaceutics* 417 (2011) 280–290.
- [47] M. Ringer, What is principal component analysis? *Nature Biotechnology* 26 (2008) 303–304.
- [48] R.V. Haware, I. Tho, A. Bauer-Brandl, Multivariate analysis of relationships between material properties, process parameters and tablet tensile strength for α -lactose monohydrates, *European Journal of Pharmaceutics and Biopharmaceutics* 73 (2009) 424–431.
- [49] M. Kubista, B. Sjögreen, A. Forootan, R. Sindelka, J. Jonák, J.M. Andrade, Real-time PCR gene expression profiling, *European Pharmaceutical Review* 1 (2007) 56–60.
- [50] S.K. Singh, P.R.P. Verma, B. Razdan, Development and characterization of a lovastatin loaded self-microemulsifying drug delivery system, *Pharmaceutical Development and Technology* 15 (2010) 469–483.
- [51] X. Dai, J.G. Moffat, J. Wood, M. Reading, Thermal scanning probe microscopy in the development of pharmaceuticals, *Advanced Drug Delivery Reviews* 64 (2012) 449–460.
- [52] A. Cutrignelli, A. Lopedota, A. Trapani, G. Boghetich, M. Franca, N. Denora, V. Laquintana, G. Trapani, Relationship between dissolution efficiency of oxazepam/carrier blends and drug and carrier molecular descriptors using multivariate regression analysis, *International Journal of Pharmaceutics* 358 (2008) 60–68.
- [53] X.J. Chen, W. Miao, Y. Liu, Y.F. Shen, W.S. Feng, T. Yu, Y.H. Yu, Microcalorimetry as a possible tool for phylogenetic studies of tetrahymena, *Journal of Thermal Analysis and Calorimetry* 84 (2006) 429–433.
- [54] D. Xu, N. Redman-Furey, Statistical cluster analysis of pharmaceutical solvents, *International Journal of Pharmaceutics* 339 (2007) 175–188.
- [55] L.X. Liu, I. Marziano, A.C. Bentham, J.D. Litster, E.T. White, T. Howes, Effect of particle properties on the flowability of ibuprofen powders, *International Journal of Pharmaceutics* 362 (2008) 109–117.
- [56] R.B. Cattell, The scree test for the number of factors, *Multivariate Behavioral Research* 1 (1966) 245–276.
- [57] H.F. Kaiser, The application of electronic computers to factor analysis, *Educational and Psychological Measurement* 20 (1960) 141–151.
- [58] M. Zhu, A. Ghodsi, Automatic dimensionality selection from the scree plot via the use of profile likelihood, *Computational Statistics & Data Analysis* 51 (2006) 918–930.
- [59] M. Gohel, M. Patel, A. Amin, R. Agrawal, R. Dave, N. Bariya, Formulation design and optimization of mouth dissolve tablets of nimesulide using vacuum drying technique, *AAPS PharmSciTech* 5 (2004) 1–6.
- [60] A.F. Faria, L.F. Marcellos, J.P. Vasconcelos, M.V.N. de Souza, A.L.S. Júnior, W.R. do Carmo, R. Diniza, M.L.A. de Oliveira, Ethambutol analysis by copper complexation in pharmaceutical formulations: spectrophotometry and crystal structure, *Journal of the Brazilian Chemical Society* 22 (2011) 867–874.
- [61] A.S. Zidan, M. Mokhtar, Multivariate optimization of formulation variables influencing flurbiprofen proniosomes characteristics, *Journal of Pharmaceutical Sciences* 100 (2011) 2212–2221.
- [62] R. Mashru, V. Sutariya, M. Sankalia, J. Sankalia, Transbuccal delivery of lamotrigine across porcine buccal mucosa: in vitro determination of routes of buccal transport, *Journal of Pharmacy and Pharmaceutical Sciences* 8 (2005) 54–62.
- [63] N. Jadhav, A. Pawar, A. Paradkar, Effect of drug content and agglomerate size on tableability and drug release characteristics of bromhexine hydrochloride-talc agglomerates prepared by crystallo-co-agglomeration, *Acta Pharmaceutica* 60 (2010) 25–38.
- [64] P. Ribardiere, G. Tchoreloff, F. Puisieux, Modification of ketoprofen bead structure produced by the spherical crystallization technique with a two-solvent system, *International Journal of Pharmaceutics* 144 (1996) 195–207.
- [65] S. Pattnaik, K. Swain, A. Bindhani, S. Mallick, Influence of chemical permeation enhancers on transdermal permeation of alfuzosin: an investigation using response surface modeling, *Drug Development and Industrial Pharmacy* 37 (2011) 465–474.
- [66] P. Roy, A. Shahiwala, Statistical optimization of ranitidine HCl floating pulsatile delivery system for chronotherapy of nocturnal acid breakthrough, *European Journal of Pharmaceutical Sciences* 37 (2009) 363–369.
- [67] I.M.F. Wouters, D. Geldart, Characterizing semi-cohesive powders using angle of repose, Particle and Particle Systems Characterization 13 (1996) 254–259.
- [68] J.L.S. Sobrinho, L.N.A. Lima, D.C. Perrelli, J.L. da Silva, F.P.M. de Medeiros, M.F. La Roca Soares, P.J. Rolim Neto, Development and in vitro evaluation of tablets based on the antichagasic benzimidazole, *Brazilian Journal of Pharmaceutical Sciences* 44 (2008) 383–389.
- [69] L.E. Holman, The compaction behaviour of particulate materials. An elucidation based on percolation theory, *Powder Technology* 66 (1991) 265–280.
- [70] W. Chen, S.G. Malghan, Investigation of compaction equations for powders, *Powder Technology* 81 (1994) 75–81.
- [71] V. Busignies, V. Mazel, H. Diarra, P. Tchoreloff, Prediction of the compressibility of complex mixtures of pharmaceutical powders, *International Journal of Pharmaceutics* 436 (2012) 862–868.
- [72] B.S. Barot, P.B. Parejija, T.M. Patel, R.K. Parikh, M.C. Gohel, Compactibility improvement of metformin hydrochloride by crystallization technique, *Advanced Powder Technology* 23 (2012) 814–823.
- [73] A. Nokhodchi, M. Maghsoodi, D. Hassan-zadeh, B. Jalali, Preparation of agglomerated crystals for improving flowability and compactibility of poorly flowable and compactible drugs and excipients, *Powder Technology* 175 (2007) 73–81.
- [74] A.B. Joshi, S. Patel, A.M. Kaushal, A.K. Bansal, Compaction studies of alternate solid forms of celecoxib, *Advanced Powder Technology* 21 (2010) 452–460.
- [75] N. Patra, S.P. Singh, P. Hamd, M. Vimladevi, A systematic study on micromeritic properties and consolidation behavior of the *terminalia arjuna* bark powder for processing into tablet dosage form, *International Journal of Pharmaceutical Excipients* 6 (2007) 6–7.
- [76] Y. Kawashima, Development of spherical crystallization technique and its application to pharmaceutical systems, *Archives of Pharmacol Research* 7 (1984) 145–151.
- [77] J.A. Hersey, J.E. Rees, Deformation of particles during briquetting, *NPhS* 230 (1971) 96.
- [78] Y. Kawashima, M. Imai, H. Takeuchi, H. Yamamoto, K. Kamiya, Development of agglomerated crystals of ascorbic acid by the spherical crystallization technique for direct tableting, and evaluation of their compactibilities, *KONA* 20 (2002) 251–262.
- [79] R.J. Roberts, R.C. Rowe, The compaction of pharmaceutical and other model materials – a pragmatic approach, *Chemical Engineering Science* 42 (1987) 903–911.
- [80] P. Paroren, M. Juslin, Compressional characteristics of four starches, *Journal of Pharmacy and Pharmacology* 35 (1983) 627–635.
- [81] C.W. Lin, T.M. Chain, Compression behavior and tensile strength of heat-treated polyethylene glycols, *International Journal of Pharmaceutics* 118 (1995) 169–179.
- [82] Y. Kawashima, M. Imai, H. Takeuchi, H. Yamamoto, K. Kamiya, Development of agglomerated crystals of ascorbic acid by the spherical crystallization techniques, *Powder Technology* 130 (2003) 283–289.
- [83] H. Leuenberger, The compressibility and compactibility of powder systems, *International Journal of Pharmaceutics* 12 (1982) 41–55.
- [84] W. Jetzer, H. Leuenberger, H. Sucker, The compressibility and compactibility of pharmaceutical powders, *Pharmaceutical Technology* 7 (1983) 33–39.
- [85] Y. Kawashima, F. Cui, H. Takeuchi, T. Niwa, T. Hino, K. Kiuchi, Improvements in flowability and compressibility of pharmaceutical crystals for direct tableting by spherical crystallization with a two solvent system, *Powder Technology* 78 (1994) 151–157.
- [86] N. Motlekar, B. Youan, Optimization of experimental parameters for the production of LMWH-loaded polymeric microspheres, *Drug Design, Development and Therapy* 2 (2008) 39–47.
- [87] US Pharmacopoeia National Formulary, USP XXIII NF XVIII, 1994.
- [88] M. Jamrogiewicz, Application of the near-infrared spectroscopy in the pharmaceutical technology, *Journal of Pharmaceutical and Biomedical Analysis* 66 (2012) 1–10.
- [89] A.A.H. Sathali, V. Selvaraj, Enhancement of solubility and dissolution rate of racecadotril by solid dispersion methods, *Journal of Current Chemical & Pharmaceutical Sciences* 2 (2012) 209–225.
- [90] K. Florey, *Analytical Profiles of drug Substances*, Academic Press, Inc., San Diego, California, 1990.
- [91] M. Palanisamy, J. Khanam, Cellulose-based matrix microspheres of prednisolone inclusion complex: preparation and characterization, *AAPS PharmSciTech* 12 (2011) 388–400.
- [92] M.K. Das, K.R. Rao, Microencapsulation of zidovudine by double emulsion solvent diffusion technique using ethyl cellulose, *Indian Journal of Pharmaceutical Sciences* 69 (2007) 244–250.
- [93] A. Modi, P. Tayade, Enhancement of dissolution profile by solid dispersion (kneading) technique, *AAPS PharmSciTech* 7 (2005) E1–E6.
- [94] P. Leppek, W. Sawicki, K. Wlodarski, Z. Wojnarowska, M. Paluch, L. Guzik, Effect of amorphization method on telmisartan solubility and the tableting process, *European Journal of Pharmaceutics and Biopharmaceutics* 83 (2013) 114–121.
- [95] P. Varlashkin, Approaches to quantification of amorphous content in crystalline drug substance by powder X-ray diffraction determination of crystallinity, *American Pharmaceutical Review* (January–February 2011) 22–28.
- [96] N.B. Naidu, K.P.R. Choudary, K.V.R. Murthy, V. Satyanarana, A.R. Hayman, G. Becket, Physicochemical characterization and dissolution properties of meloxicam-cyclodextrin binary systems, *Journal of Pharmaceutical and Biomedical Analysis* 35 (2004) 75–86.
- [97] N.S. Murthy, Recent developments in polymer characterization using X-ray diffraction, *The Rigaku Journal* 21 (2004) 15–24.
- [98] N. Terinte, R. Ibbett, K.C. Schuster, Overview on native cellulose and microcrystalline cellulose structure studied by X-ray diffraction (WAXD): comparison between measurement techniques, *Lenzinger Berichte* 89 (2011) 118–131.
- [99] C.S. Randall, W.L. Rocco, P. Ricou, XRD in pharmaceutical analysis: a versatile tool for problem-solving, *American Pharmaceutical Review* (September–October 2010) 52–59.

- [100] M. Jaboyedoff, F. Bussy, B. Kubler, P. Thelin, Illite "crystallinity" revisited, *Clays and Clay Minerals* 49 (2001) 156–167.
- [101] M. Jbilou, A. Ettabia, A. Guyot-Hermann, J.C. Guyot, Ibuprofen agglomerates preparation by phase separation, *Drug Development and Industrial Pharmacy* 25 (1999) 297–305.
- [102] N. Rasenack, B.W. Muller, Properties of ibuprofen crystallized under various conditions: a comparative study, *Drug Development and Industrial Pharmacy* 28 (2002) 1077–1089.
- [103] V.R. Gupta, S. Mutalik, M.M. Patel, G.K. Jani, Spherical crystals of celecoxib to improve solubility, dissolution rate and micromeritic properties, *Acta Pharmaceutica* 57 (2007) 173–184.
- [104] C. Cheng, S. Liu, B.J. Mueller, Z. Yan, A generic static headspace gas chromatography method for determination of residual solvents in drug substance, *Journal of Chromatography A* 1217 (2010) 6413–6421.
- [105] ICH Q3C (R5), Impurities: Guideline for Residual Solvents. , Available from: http://www.ema.europa.eu/docs/en_GB/document_library/Scientific_guideline/2011/03/WC500104258.pdf February 2011.
- [106] European Pharmacopoeia, Directorate for the Quality of Medicines of the Council of Europe, Strasbourg, 5th ed., 2005.
- [107] A.R. Paradkar, A.P. Pawar, J.K. Chordiya, V.B. Patil, A.R. Ketkar, Spherical crystallization of celecoxib, *Drug Development and Industrial Pharmacy* 28 (2002) 1213–1220.
- [108] K. Garala, J. Patel, A. Dhingani, M. Raval, A. Dharamsi, Overcoming limitations in dissolution testing of poorly water soluble racecadotril, *Inventi Rapid: Pharm Tech* 2012 (2013) 1–4.
- [109] P.G. Bhole, V.R. Patil, Enhancement of water solubility of felodipine by preparing solid dispersion using poly-ethylene glycol 6000 and poly-alcohol, *Asian Journal of Pharmaceutics* 3 (2009) 240–244.